DISSERTATIONES BIOLOGICAE UNIVERSITATIS TARTUENSIS
175

DISSERTATIONES BIOLOGICAE UNIVERSITATIS TARTUENSIS
175

EERO TALTS

Photosynthetic cyclic electron transport – measurement and variably proton-coupled mechanism

TARTU UNIVERSITY
PRESS

Faculty of Science and Technology, University of Tartu, Tartu, Estonia

Dissertation is accepted for the commencement of the degree of Doctor of Philosophy (PhD) in Plant Physiology on January 29, 2010 by the Council of the Institute of Molecular and Cell Biology, Faculty of Science and Technology, University of Tartu.

Supervisors: PhD. Agu Laisk
University of Tartu,
Tartu, Estonia

Knd. Vello Oja
University of Tartu,
Tartu, Estonia

Opponent: Senior lecturer (PhD) Giles Johnson,
Faculty of Life Sciences,
University of Manchester, UK

Commencement will take place at the Institute of Molecular and Cell Biology, Riia 23, Tartu, on March 12, 2010 at 14.00.

ISSN 1024–6479
ISBN 978–9949–19–310–3 (trükis)
ISBN 978–9949–19–311–0 (PDF)

Tartu Ülikooli Kirjastus
www.tyk.ee
Tellimus nr. 49

CONTENTS

LIST OF ORIGINAL PUBLICATIONS

Current thesis is based on the following original publications which will be referred by their Roman numerals:

I. **Talts**, **E.,** Oja, V., Rämma, H., Rasulov, B., Anijalg, A. and Laisk A. (2007) "Dark inactivation of ferredoxin-NADP reductase and cyclic electron flow under far-red light in sunflower leaves." Photosynth Res **94**:109–120.

II. Laisk, A., **Talts**, **E.,** Oja, V., Eichelmann, H., and Peterson, R.B. (2010) "Fast cyclic electron transport around photosystem I in leaves under far-red light: a proton-uncoupled pathway?" Photosynth Res **103**:79–95.

III. Laisk, A., Eichelmann, H., Oja, V., **Talts E.,** and Scheibe, R. (2007) "Rates and roles of cyclic and alternative electron flow in potato leaves." Plant Cell Physiol **48(11)**:1575–588.

Articles are reprinted with the permission of copyright owners.

My contributions to the articles:
Ref. I: I performed majority of experiments and data analysis, and participated in the writing of the manuscript.
Ref. II: I performed majority of experiments and data analysis, and participated in the writing of the manuscript.
Ref. III: I participated in experiments and data analysis.

LIST OF ABBREVIATIONS

ADP	–	Adenosine DiPhosphate
ATP	–	Adenosine TriPhosphate
BPG	–	1,3-BisPhosphoGlycerate
CET	–	Cyclic Electron Transport
Cyt	–	Cytochrome
e^-	–	electron
ECS	–	ElectroChromicShift
ETR	–	Electron Transport Rate
Fd	–	Ferredoxin
FNR	–	Ferredoxin-NADP Reductase
FRL	–	Far-Red Light
G3P	–	Glyceraldehyde 3-Phosphate
ISP	–	Iron-Sulphur Protein
LET	–	Linear Electron Transport
NADP	–	Nicotinamide Adenine Dinucleotide Phosphate
P680	–	Donor pigment of PSII
P700	–	Donor pigment of PSI
PC	–	PlastoCyanin
PFD, PAD	–	Photon Flux Density, incident and absorbed
PGA	–	3-PhosphoGlycerate
P_i	–	phosphate
PQ	–	PlastoQuinone
PSI, PSII	–	PhotoSystem I and PhotoSystem II
WL	–	White Light

1. INTRODUCTION

Adenosine triphosphate (ATP) is an important energetic cofactor for "pushing" metabolic biochemical pathways in the necessary direction. In heterotrophic cells ATP is regenerated by phosphorylating ADP in mitochondria as a result of a complex system of reactions where molecular oxygen is reduced to water with the help of electrons obtained at the expense of oxidation of organic compounds, mostly sugars. There is a certain stoichiometry between the number of electrons transferred from the sugars to oxygen and the number of ATP formed. The stoichiometry has not yet been unequivocally defined, however, it has little principal importance for the metabolic pathways since different stoichiometries simply mean different amounts of sugars have to be oxidized and oxygen reduced for supporting a certain metabolic pathway. The availability of oxygen as the electron acceptor is not limited, as well as sugars are usually abundant for respiration.

Photosynthesis is a metabolic pathway that produces organic compounds using energy from sunlight – a reversed process compared to respiration. In photosynthesis, water is oxidized at the expense of light energy releasing molecular oxygen and protons. The electrons from water are transported to carbon dioxide that is reduced to form sugars. Four electrons are used per reduction of 1 CO_2. The reduction occurs in a complex sequence of reactions requiring also 3 ATP per CO_2 reduced (the Calvin-Benson Cycle). Different from other cellular metabolism, the reduction of CO_2 cannot be supported by ATP generated in mitochondrial respiration, because photosynthesis is a very fast process that would require fast reoxidation of too much sugar to support itself. Instead, the synthesis of ATP is powered by the same flow of electrons that are heading from water to CO_2, without the involvement of mitochondrial ATP synthesis. In photosynthesis a strict stoichiometry is absolutely necessary between the electron flow and ATP synthesis, because, differently from mitochondria, where O_2 is an unlimited electron acceptor, the reduction of a CO_2 molecule needs exactly 3 ATP to complete the synthesis of (a single carbon moiety in) sugar.

The synthesis of ATP from ADP + P_i occurs in ATP synthase, an amazing molecular machine powered by protons flowing through its turbine situated in a biomembrane. The energy forcing the protons through the ATP synthase comes from the difference of H^+ concentrations (pH difference, ΔpH) and the difference in electrical potential at the two sides of the membrane – generally called the proton motive power, pmf. Such membrane "energization" is supported by the electrons flowing from H_2O to CO_2. One H^+/e^- is released during water oxidation, but $2H^+/e^-$ are translocated additionally during a specifically organized transport pathway called the "Q-cycle". As a result of this $3H^+/e^-$ are translocated from chloroplast stroma through the thylakoid membrane into the lumen during the photosynthetic electron flow. Altogether $12H^+/4e^-$ are translocated through the membrane during the reduction of 1 CO_2 and release of 1 O_2.

The question how many H^+ are passing through the synthase per ATP has been subject to discussions, but very recent data indicate that $4H^+$/ATP is the requirement (Steigmiller et al. 2008), which means that exactly 3ATP are synthesized per CO_2 reduced. This would mean there are no ATP/e^- stoichiometry problems during photosynthesis. However, since there are no other ATP sources in chloroplasts in the light than that based on the photosynthetic electron transport, the 3ATP/$4e^-$ stoichiometry may still be violated if some of the chloroplast ATP is used for other reactions than the primary CO_2 reduction to the level of sugars – e.g. for starch and protein synthesis. Therefore, the problem of regulation of the exact ATP/e^- stoichiometry remains actual, though only in a smaller scale than assumed before. The results of the work presented in this dissertation contribute to the progress in this direction, showing that one possible pathway of additional ATP synthesis – the cyclic photophosphorylation – is not as important as usually assumed, but alternative electron acceptors like N and O_2 reduction become important in this respect.

2. REVIEW OF LITERATURE

2.1. Photosynthetic Electron Transport Chain

In plants the photosynthetic process occurs in chloroplasts, which are small organelles (about 5 micrometers across). The chloroplast is surrounded by two membranes, an outer envelope membrane and an inner envelope membrane (Fig. 1). A complex membrane system – called thylakoids – is filling a part of the internal space of the chloroplasts (only a fragment of a thylakoid is shown enlarged in Fig. 1). The rest of the internal space is called stroma. Photosynthetic process can be formally divided into two parts: light reactions and dark reactions. The light reactions are carried out by proteins and pigment-protein complexes bound to the thylakoid membranes. They involve two truly light-dependent photoreactions associated to Photosystem II and Photosystem I (denoted PSII and PSI). Other carriers are involved in electron transport to and away from the photosystems (scaled in redox potentials in Fig. 2). The water splitting complex donates electrons to PSII, a mobile electron carrier plastoquinol/plastoquinone (PQH_2/PQ) carries electrons from PSII to the proton-transporting Cytochrome b_6f complex (Cyt b_6f), another mobile electron carrier plastocyanin (PC) carries electrons from Cyt b_6f to PSI. Ferredoxin (and ferredoxin-NADP reductase) carries electrons from the acceptor side of PSI to NADP. The latter is directly involved in carbon reduction, thus being considered as "end product" of the light reactions.

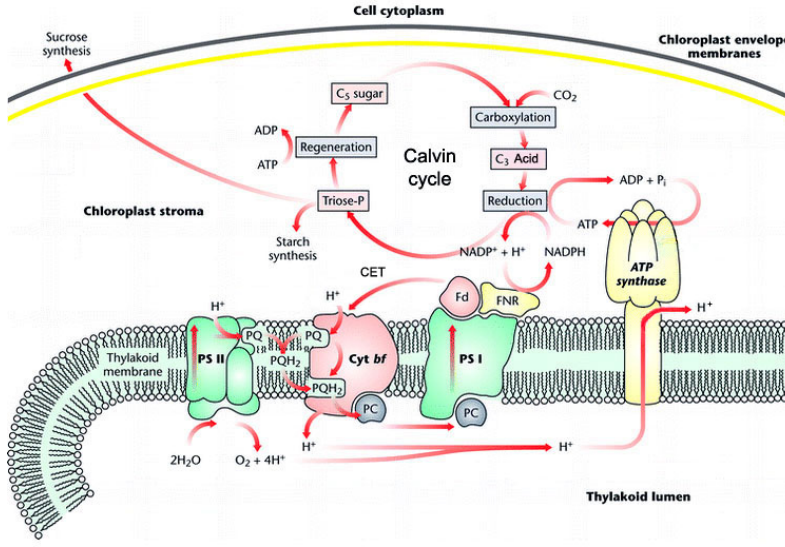

Figure 1. general scheme of processes in chloroplast. CET – Cyclic Electron Transport; PSI and PSII – Photosystems I and II; PQ and PQH_2 – plastoquinone/plastoquinol; Cyt *bf* – Cytochrome b_6f complex; PC – Plastocyanin; Fd – Ferredoxin; FNR – Ferredoxin-NADPH reductase.

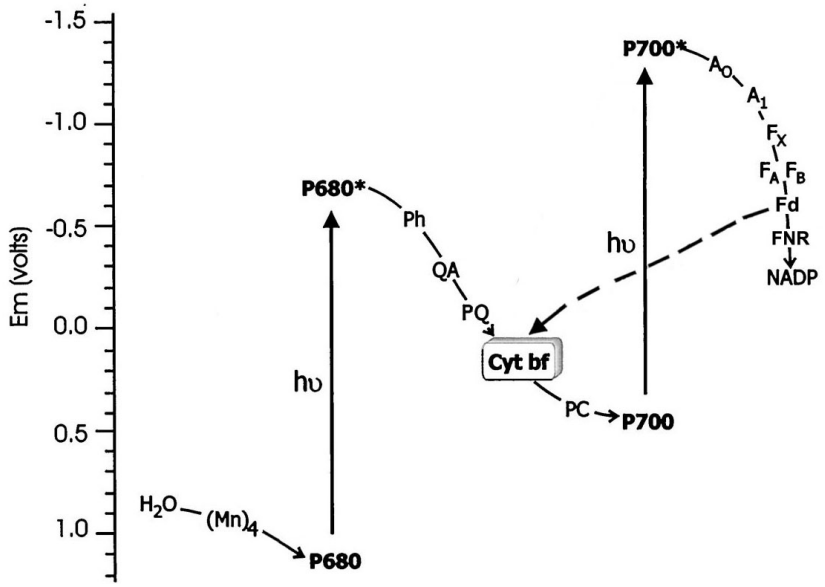

Figure 2. The electron transport pathway in redox potential scale. Solid line – linear electron pathway. Dashed line – cyclic electron transport. $(Mn)_4$ – water splitting complex; P680 – reaction centre of PSII; Ph – pheophytin; QA – quinone type electron acceptor; PQ – plastoquinone; Cyt *bf* – cytochrome b_6f complex; PC – plastocyanin. P700 – reaction centre of PSI; A0, A1, FX, FA, FB – electron carriers in PSI complex; Fd – ferredoxin; FNR – ferredoxin-NADPH reductase; NADP – nicotinamide adenine dinucleotide phosphate. Adapted from (Hillier and Babcock 2001).

2.1.1. Photosystem II and water splitting

The photosynthetic electron transport begins with water splitting in the oxygen evolving complex at PSII (Barber 1998; Buchanan, B.B., Gruissem, W., and Jones, R.L. 2000; Hillier et al. 2001). In the oxygen evolving complex electrons are extracted from water, excited by light energy and directed to reduce PQ. PSII is a dimeric transmembrane protein cluster composed of 20 subunits, plus the accessory light harvesting antenna chlorophyll-binding proteins. Each PSII contains numerous cofactors: chlorophyll a, beta-carotene, integral lipids, plastoquinone etc. (Guskov et al. 2009). An important component of PSII is the reaction centre pigment P680, which is a dimer of two chlorophyll molecules. This pigment pair is placed near the lumenal side of the membrane (Fig. 3). The absorption of a photon transfers P680 into its excited state (from +1.12 to – 0.81 V in redox scale). The excited electron passes on to pheophytin and further to a bound quinone type acceptor Q_A close to the stromal side of the membrane (E_m about 0 V). The formed $P680^+$ is a strong oxidizer, able to withdraw an electron from the Mn cluster of the water splitting complex. The latter accumulates four

electron “holes” and then becomes re-reduced by accepting four electrons from two H_2O (Kok et al. 1970). Residual oxygen radicals combine to form the diatomic O_2 molecule that is released into thylakoid lumen. The reaction requires the energy of four photons per one oxygen molecule. In this way, pheophytin accepts electrons from P680 and passes them on to a PQ molecule (Q_A), tightly associated with the reaction centre. The Q_A^- quinone passes its electron on to a second PQ molecule (Q_B) that can leave the binding site and freely diffuse in the membrane (quinones are hydrophobic compounds that diffuse between lipids inside the biomembranes). Plastoquinone at the Q_B-site differs from Q_A in that it works as a two-electron acceptor, and becomes fully reduced and protonated after two photochemical turnovers of the reaction centre.

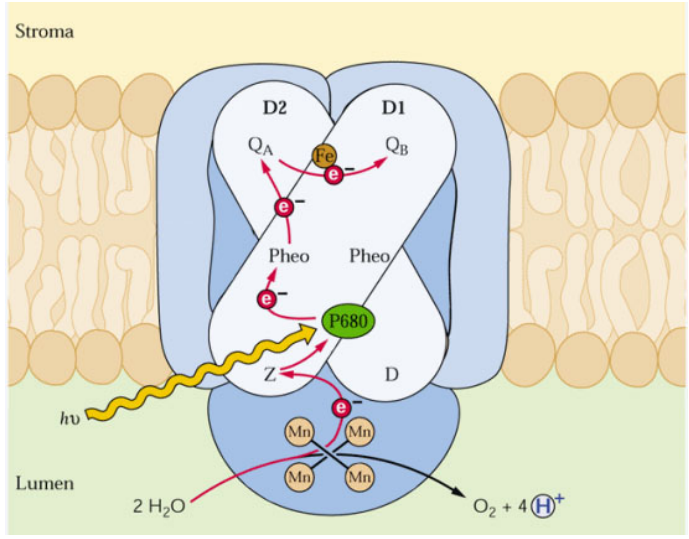

Figure 3. Electron movement in PSII complex.

2.1.2. Plastoquinone, plastoquinol

Plastoquinone (PQ) is a lipid-soluble benzoquinone derivative with an isoprenoid side chain which is involved in the photosynthetic electron transport (Buchanan, B.B., Gruissem, W., and Jones, R.L. 2000). The double reduction of PQ and the formation of plastoquinol (PQH_2) at the Q_B site of PSII is accompanied by the capture of two protons (H^+) from the stromal matrix of the chloroplast. The reduced plastoquinone PQH_2 then unbinds from the reaction centre and diffuses in the hydrophobic core of the membrane. Simultaneously an oxidized PQ finds its way to the Q_B-binding site and the process is repeated (there are about 10 PQ/PQH_2 per PSII in the membrane). Several compounds can inhibit electron transport by binding at or near the Q_B-site, preventing

access to plastoquinone. These Q_B-site inhibitors have been extremely useful for investigating PSII function, and some are important commercial herbicides (like DCMU, Atrazine, Simazine, Fenuron, ec.) (Breton et al. 2006). The mobility of the PQ in the membrane allows a single PSII reaction centre to interact with a number of Cytochrome b_6f complexes (Hauska et al. 1996).

2.1.3. Cytochrome b_6f and Q-cycle

The Cytochrome b_6f (Cyt b_6f) is a 220 kDa symmetric dimeric complex which transfers electrons from PSII to PSI by catalyzing the oxidation of PQH_2 and the reduction of plastocyanin (PC). The transfer of electrons from PQH_2 to PC (and further to PSI) is coupled with the release of H^+ into the lumenal space of the thylakoid membranes. As a result of this 1 H^+/e^- are translocated across the membrane from the stromal to the lumenal side, coupled with the reduction and oxidation of PQ/PQH_2 during the photosynthetic electron transport (Hauska et al. 1996). In addition to this, an amazing molecular machine called Q-cycle (Mitchell 1966; Mitchell 1975a) repeats the process, translocating another H^+, so that $2H^+/e^-$ is the total stoichiometry of e^-/H^+ transfer through the Cyt b_6f complex.

The operation of the Q-cycle is based on the molecular symmetry of quinones. Both states, either double reduced or double oxidized are stable, but the single-oxidized state is a strong reductant or oxidant. At Cyt b_6f the process of PQH_2 oxidation is organized so that the first electron is accepted by a stronger oxidant Cyt f (and further on by PC and $P700^+$ of PSI, see Fig. 4). The oxidation of PQH_2 occurs in a "positive" or p-site at the lumenal side of the membrane. There are two, but rather weak oxidants Cyt b available for the second electron, but the energetic barrier is easily overcome due to the molecular asymmetry of the singly reduced PQ^-. This way each PQH_2 is oxidized sending one e^- to Cyt f and further on to PS I, but the second electron is going to one of the two Cyt b hemes. After two PQH_2 have been oxidized this way, the two low-potential Cyt b send their electrons – simultaneously or via the intermediate semiquinone state – to an oxidized PQ. This reduction of PQ takes place at a site near the stromal side of the membrane (called n-site from "negative"), so that the coupled protons are captured from the stroma. The reduced PQH_2 leaves the site and moves to the p-site, where it is oxidized, leaving one e^- to Cyt f and the second to Cyt b again. As we see, every act of PQH_2 oxidation releases one electron to PSI, but forces the second electron to repeat the H^+ -coupled Q-cycle. On average, every e^- passes through the Cyt b_6f complex twice, cotranslocating $2H^+/e^-$. Since e^- transfer through Cyt b_6f is closely related to the Cyclic Electron Transport – the topic of this dissertation – we shall return to it in more details below.

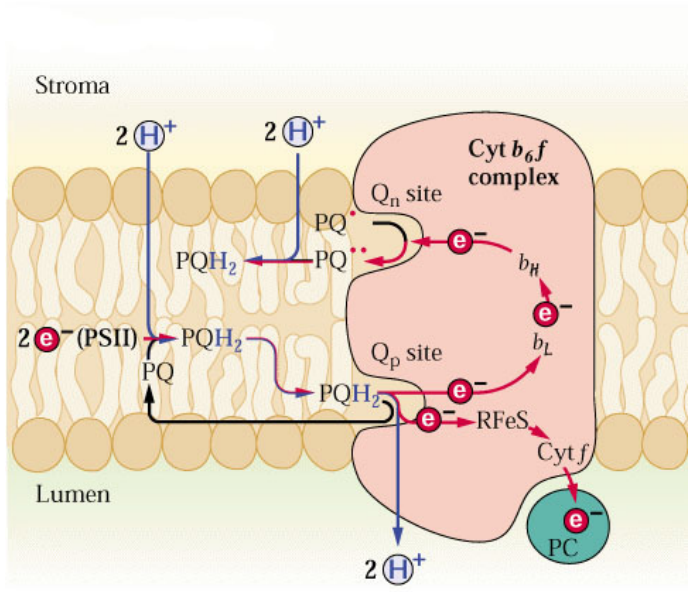

Figure 4. Q-cycle and electron movement in $CytB_6F$ complex.

2.1.4. Plastocyanin

The overview of plastocyanin is based on(Silva de D.G.A.H. et al. 1992; Gupta et al. 2002; Musiani et al. 2005). Plastocyanin accepts an e^- from Cyt f, diffuses to PS I and transfers the e^- to $P700^+$, the donor pigment of PSI. Plastocyanin (PC) is a 10.5 kDa monomeric copper-containing protein. In order to prevent direct e^- transfer from PQH_2 to PC passing by the Cyt b_6f, PC operates in the inner aqueous phase of the thylakoid lumen, while PQH_2 does that in the lipid membrane. PC contains a copper ion that is ligated to four residues of the polypeptide. The copper ion serves as a one-e^- carrier with a midpoint potential of +370 mV, near that of heme f.

2.1.5. Photosystem I

Photosystem I (PSI) is the second of the two sequential photochemical steps in photosynthesis (Haldrup et al. 1999; Sawaya and Merchant 2005; Nelson and Yocum 2006). Its operation principles are similar to those of PSII, but some differences are noteworthy. PSI contains more protein subunits than PSII. Its molecular weight is 525 kDa without the antenna complex, plus 150 kDa of the chlorophyll-protein antenna subunits (Fig. 5). The crystal structure of the complete PSI from a higher plant (4.4 Å resolution) has been determined (Ben-

Shem et al. 2003). Its intricate structure shows 12 core subunits, 4 different light-harvesting membrane proteins assembled in a half-moon shape on one side of the core, 45 transmembrane helices, 167 chlorophylls, Fe_4S_4 clusters and 2 phylloquinones. About 20 chlorophylls are positioned in strategic locations in the cleft between LHCI and the core. In plants, the PSI complex catalyzes the oxidation of PC and the reduction of ferredoxin (Fd). As in PSII, two polypeptides, subunit A and subunit B, form a heterodimer that bind the primary electron donor and acceptor and the transmembrane electron carriers. The primary donor, P700, is chlorophyll dimer, and the primary acceptor, A_0, a duplicated chlorophyll monomer. As in PSII, a quinone (phylloquinone, vitamin K1), operates as a single electron acceptor (A_1, also duplicated). Then electrons are transferred from A_1 to a Fe_4S_4 cluster (F_X) that is ligated to both polypeptides of the heterodimer. An extrinsic protein, subunit C, containing two Fe_4S_4 clusters, F_A and F_B, is located on the stromal side of the reaction centre close to F_X and electron transfer goes from F_X to F_B through F_A and then from F_B to Fd.

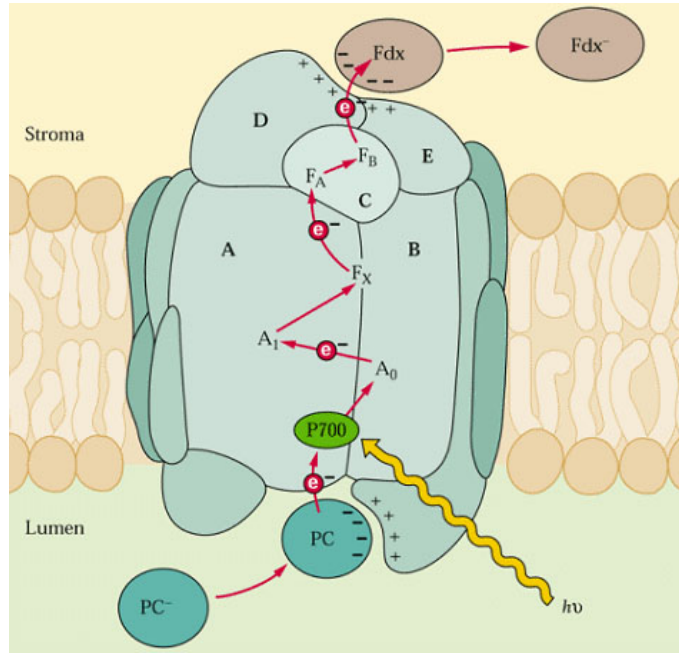

Figure 5. Electron movement in PSI complex.

2.1.6. Ferredoxin

Ferredoxin (Fd) is a small (ca. 11 kDa) iron-sulphur protein that mediates electron transfer between PSI and Ferredoxin-$NADP^+$ oxidoreductase (Fukuyama 2004; Hanke et al. 2004; Hase et al. 2006). There are about 6–8 Fd per PSI, operating in the stromal aqueous phase of the chloroplast. The Fe_2S_2 cluster, ligated by four cysteine residues, serves as a one-electron carrier. Ferredoxin has the distinction of being one of the strongest soluble reductants found in cells (–420 mV). Plants contain different forms of ferredoxin, all of which are encoded in the nuclear genome. Fd is an important branching point between several electron transport pathways, enabling transfer of electrons to the Calvin-Benson cycle of CO_2 reduction, nitrite reduction, sulphite reduction, glutamate synthase, thioredoxin reductase, Mehler type reduction of molecular oxygen and, finally, PSI cyclic electron transport (Neuhaus and Emes 2000). Ferredoxin may also be in complex with Ferredoxin-$NADP^+$ oxidoreductase and PSI.

2.1.7. Ferredoxin-$NADP^+$ oxidoreductase

Ferredoxin-$NADP^+$ oxidoreductase (FNR) links Fd (as one-electron donor) to the two-electron acceptor $NADP^+$(Clark et al. 1984; Zhang et al. 2001; Hanke et al. 2004; Hase et al. 2006). The electron carrier in FNR is flavin adenine dinucleotide (FAD) which, under equilibrium conditions, is a two-electron acceptor with E_m near –360 mV at pH 7 (Karplus and Faber 2004). For catalytic activity, two molecules of Fd must donate electrons to FNR, which in turn reduces $NADP^+$ to NADPH. FNR is a single polypeptide (ca. 35 kDa) which is encoded by a nuclear gene. A part of FNR is soluble in the stromal phase, but a part of it is found bound to different peptides at the stromal side of the photosynthetic membrane, mainly to Cyt b_6f and to PSI, where it operates as a peripheral protein (Carrillo and Vallejos 1982; Ruhle et al. 1988). The three-dimensional structure of spinach FNR has been determined at 1.7 Å resolution (Burns and Karplus 1994). It appears that Fd and $NADP^+$ bind to FNR at two different domains. The redox enzyme FNR has been shown to be activated by light and inactivated in the dark within a few minutes *in vivo* (Ruhle et al. 1988; Shin 2004; Talts et al. 2007). The light-activation of FNR happens via the protein-mediated thioredoxin system and leads to conformational changes. This requires electrons from Fd which reduce disulfide-bonds of thioredoxin as the step of activation (Buchanan, B.B., Gruissem, W., and Jones, R.L. 2000). As with Fd, the FNR can be found as a subunit of the chloroplast Cyt b_6f complex also.

2.1.8. NADP

The final electron acceptor in the photosynthetic electron transport chain is $NADP^+$, which is fully reduced by two electrons (and one proton) to form NADPH. NADPH is a strong reductant (E_m = –320 mV at pH 7), and it serves as a mobile electron carrier in the stromal aqueous phase of the chloroplast. Although NADPH is a powerful reductant, it reacts slowly with oxygen, which enables it to serve a stable source of electrons for the reduction of carbon dioxide, as well as in other reductive biosynthetic pathways.

2.2. ATP Synthesis

Along with producing the reductant NADPH, the energy of the light-excited electrons is also converted into the pyrophosphate bond of an ATP molecule. The latter is energetically supporting CO_2 reduction and starch synthesis in chloroplasts.

ATP synthase (ca 500 kDa, Fig. 6), is a thylakoid membrane enzyme that can synthesize ATP from ADP and inorganic phosphate (P_i) by using energy of an H^+ gradient, created by photosynthetic electron transport (Yoshida et al. 2001; Allen 2002; Hisabori et al. 2003; Richter et al. 2005; McCarty 2005). The overall structure and the catalytic mechanism of the chloroplast ATP synthase are almost the same as those of the mitochondrial enzyme. ATP synthase consists of a catalytic portion (CF_1), central and side stalks, and a thylakoid membrane-embedded part (CF_0). The latter serves for proton transport across the membrane powering the catalytic CF_1 part. The CF_1, like its mitochondrial and bacterial counterparts, is functional in ATP synthesis and sticks into stroma, where dark reactions of photosynthesis (the Calvin-Benson cycle) take place. The CF_1-part consists of three α-subunits and three β-subunits that are arranged alternately, forming an orange-like cylinder of (αβ)3 around an asymmetrical coiled-coil structure (γ-subunit), which is the central link between CF_1 and CF_0. The CF_0-part consists of symmetrically placed multiple III subunits (their number is 9–14, depending on species), two II subunits and one I subunit. Subunits δ and II dimer together forming a peripheral stalk which binds CF_0 to CF_1. This stalk is considered to act as a "stator" holding the α, β, I and III subunits still while the γ, ε subunits rotate. The III-ring is attached to the asymmetric central stalk (γ-subunit), which rotates within the (αβ)3 causing the 3 catalytic nucleotide binding sites to go through a series of conformational changes that lead to ATP synthesis.

The catalytic mechanism involves the active site of a β subunit cycling between three states. The regulation of CF_1 is accomplished by H^+ gradient and by electron transfer providing reductants that are used to reduce disulphide bridges in CF_1. ATP synthase can also act as ATPase and proton pump, hydrolyzing available ATP to ADP and P_i, and moving H^+ to lumen.

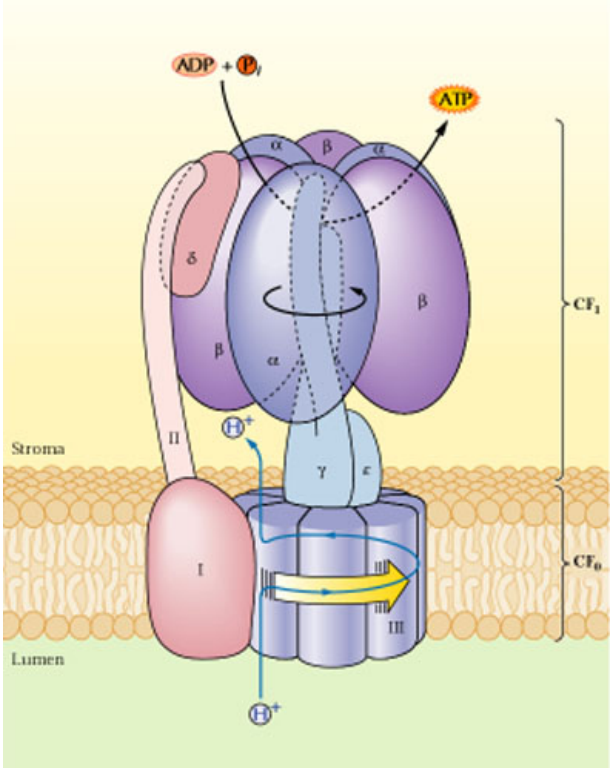

Figure 6. ATP synthase.

2.3. Carbon Fixation Cycle

The carbon fixation cycle (Calvin-Benson cycle) in the stroma of chloroplasts is accomplished by a series of light independent biochemical reactions in which carbon enters in the form of CO_2 and leaves in the form of a sugar (triose) phosphate (Bassham et al. 1950). The cycle depends on ATP as an energy source and consumes NADPH as reducing power. Three phases of the cycle may be distinguished that are described per 3 CO_2 bound.

1) In the carbon fixation phase 3 CO_2 are incorporated into three 5-C sugar bisphosphates (ribulose-1,5-bisphosphate, RuBP). The enzyme catalyzing this step is RuBP carboxylase-oxygenase (Rubisco). Due to its relatively slow site turnover, but required fast rate, it is the most abundant protein in chloroplasts and the most abundant protein on Earth as well. The formed six-carbon intermediate product is immediately split to form two 3-C molecules of 3-phosphoglycerate (PGA). Six 3-C PGA molecules are formed as a result of binding 3 CO_2.

2) In the second phase PGA is reduced and the product is formed. First, the enzyme phosphoglycerate kinase catalyses the phosphorylation of the 6 PGA by 6 ATP, forming 1,3-bisphosphoglycerate (BPGA) and ADP as the products. Then the reductive power of 6 NADPH is used to convert the 6 BPGA to 6 glyceraldehyde 3-phosphate (G3P). One of the six formed molecules is the 3-C sugar phosphate product of the cycle, which is a precursor to glucose and other sugars. The other five 3-C molecules are used for regeneration of three 5-C RuBP in phase 3. During the process 6 NADPH are oxidized to $NADP^+$ and re-reduced by the light reactions as described above.
3) The third phase is the regeneration of RuBP. It is a rather complex system of molecular conversions during which the five 3-C sugar phosphates are converted into three 5-C sugar phosphates. Three ATP are needed to convert the three 5-C monophosphates to the 5-C bisphosphates (RuBP), thereby completing the cycle. For every three molecules of CO_2 that enter the cycle, the net output is one molecule of G3P. For each G3P synthesized, the cycle spends 9 molecules of ATP and 6 molecules of NADPH, or 3 ATP and 2 NADPH per CO_2. The light reactions sustain the Calvin-Benson cycle by regenerating the ATP and NADPH.

Two G3P molecules that have exited from the cycle are used to make larger carbohydrates like fructose-6-phosphate, glucose-6-phosphate and glucose-1-phosphate. These are used to form starch in chloroplasts and sucrose in cytosol. The inorganic phosphate liberated during these processes is retransported into chloroplasts and reused for phosphorylation of ADP.

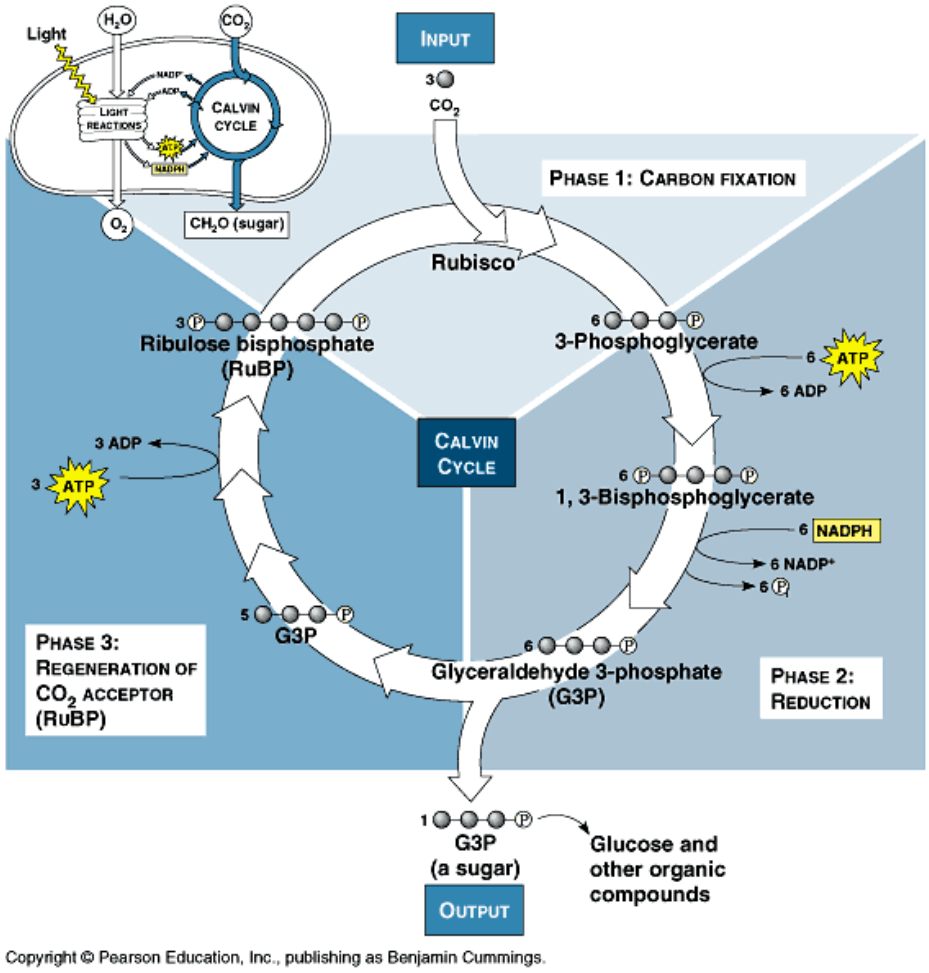

Figure 7. Carbon fixation cycle.

2.4. Stoichiometry of Electron Carriers

The stoichiometry of big transmembrane protein complexes is considered to be 1PSII:1Cyt b_6f :1PSI (Whitmarsh and Ort 1984) but controversially large variability in the ratio of PSII to PSI reaction centres (from 0.43 to 3.3) in different photosynthetic membranes is also reported (Melis and Brown 1980). In spinach chloroplasts, 7 – 8 PQ molecules were found per reaction centre of PSII and most of the plastoquinone pool was associated with the grana membranes (Melis et al. 1980; McCauley and Melis 1986). The PC pool is about 3–4 PC per PSI (Kirchhoff et al. 2004) and the ratios of Fd to FNR to PC approximated 5:3:4 per P700, as determined by immuno-electrophoresis

(Böhme 1978). The protein complexes that catalyze electron transfer and energy transduction are unevenly distributed in thylakoids: PSI is located in the stroma-exposed lamellae (where PSI : PSII > 3), PSII is found almost exclusively in the grana membranes (PSII : PSI > 2), the ATPase is located mainly in the stroma lamellae, and the Cyt b_6f complex is found in grana and grana margins (Melis et al. 1980; Albertsson 2001; Nelson et al. 2006), (Fig. 8). Therefore, it is commonly believed that grana membranes are engaged in linear electron transport (LET), but stroma lamellae are maintaining ATP synthesis by carrying out cyclic electron transport (CET).

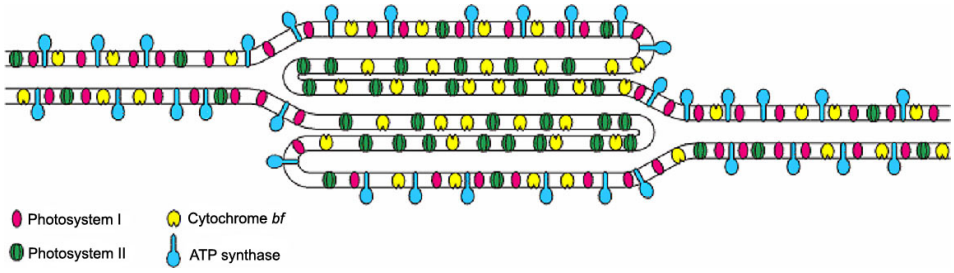

Figure 8. Location of photosynthetic complexes in thylakoids.

2.5. ATP/NADPH Stoichiometry – the Progress of Views

2.5.1. History of the concept of cyclic photophosphorylation.

Over 50 years ago (in 1954) Arnon and co-workers discovered that ATP was synthesized in illuminated chloroplasts in the absence of gas exchange, which started the long-lasting discussion about CET and the related cyclic photophosphorylation (Arnon et al. 1954). For about 25 years the only and the absolute authority of CET was Daniel Arnon with his research group. The most cited crucial experiment proving CET was carried out in 1955, where vitamin K dependent ATP synthesis in broken chloroplast membranes was demonstrated under anaerobic conditions (Arnon et al. 1955). At that time the Z-scheme was not known and photosynthesis was described with two parallel light-dependent redox flows (Fig. 9):

1) Linear flow – water is split to H and O without ATP production; O leaves the system as molecular oxygen and H reacts with CO_2 forming sugar;
2) Cyclic flow – water is split to H and O; over a series of carriers (FMN, Vitamin K, Cytochromes) H moves back to O to re-form water. This was believed to be the only process where ATP production could exist (Arnon et al. 1955; Arnon 1955). In fact, in our contemporary terms Arnon was speaking about "pseudo cyclic" phosphorylation involving re-synthesis of

water, such as e.g. the Asada's water-water cycle involving the production of ATP by the LET pathway.

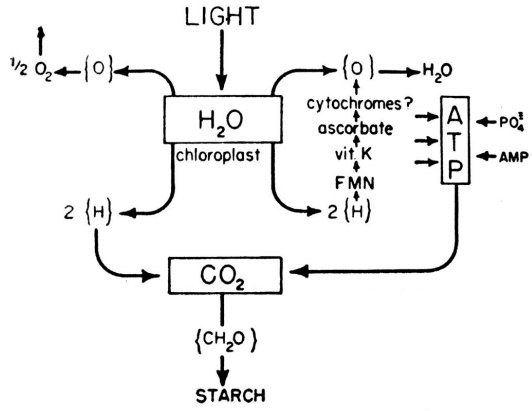

Figure 9. Scheme of photosynthesis at 50 – 60s. Compare with Fig. 1 and 2. (Arnon et al. 1955; Arnon 1955).

2.5.2. Z-scheme and the involvement of the Q-cycle

Until 1960-s, the production of ATP in photosynthesis was believed to be connected only with the cyclic photophosphorylation. The discovery of the Z-scheme (Hill and Bendall 1960) introduced new aspects into chloroplast energetic, including the necessity to relate ATP synthesis to the "non-cyclic" electron transport. Notice that in order not to devaluate CET, the novel pathway was termed "non-cyclic" (in this dissertation still termed "linear electron transport", LET). The first investigations that proved ATP production via LET were reported in 60-s. These early measurements revealed the stoichiometry of O_2:NADPH:ATP of 1:2:2 (2 H^+ per 1 e^-) (Arnon et al. 1958; Campo et al. 1968). Any amount of ATP exceeding this ratio was thought to be synthesized via CET (Arnon et al. 1958; Arnon et al. 1959; Arnon et al. 1961).

Whether the deficit in ATP (and proton) budget exists and how big it actually is has been a subject of debates since the discovery of the Z-scheme. After Peter Mitchell related ATP synthesis to the energy of transmembrane proton flux (Mitchell 1966), the budget analysis involved the coupling ratios, how many H^+/e^- in LET and how many H^+/ATP in ATP synthase? Initially the H^+/e^- ratio was believed to be 2 (one from H_2O splitting and one from PQH_2 oxidation (Campo et al. 1968). Since the experimentally obtained H^+/ATP ratio tended to be close to 3, the budget predicted 8/3 ATP could be synthesised per transport of 4 e^- instead of the necessary 9/3. This budget maintained a small deficiency of 1/3ATP, leaving a role for CET to cover the deficiency. After Peter Mitchell suggested the operation of the Q-cycle in mitochondria (Mitchell 1975a; Mitchell 1975b) the arguments focussed on whether the Q-cycle is

operating in chloroplasts also? A weighty counterargument was, if it were operating then the budget would be $12H^+/4e^-$ that would support the synthesis of 12/3 = 4 ATP instead of the necessary 3 ATP. This discrepancy remained in air for long time even after the establishment of the obligatory involvement of the Q-cycle in interphotosystem electron flow (Rich 1988). This contradiction, however, catalyzed further investigations of the H^+/ATP stoichiometry of ATP synthase.

2.5.3. Proton – ATP stoichiometry

As said above, early investigations revealed that about $3H^+$/ATP were required by ATP synthase. A breakthrough happened in 1990 when the requirement of $4H^+$/ATP was rather convincingly shown (Rumberg et al. 1990). Provided that the Q-cycle is operating ensuring the ratio of 12 H^+ per 2 NADPH (Rich 1988; Sacksteder et al. 2000) and the requirement for ATP synthase is $12H^+$/3ATP, the requirements of the Calvin cycle (3 ATP per 2 NADPH) are exactly satisfied, with this downgrading the role of cyclic phosphorylation once again. Only a small ATP deficiency may be caused by its consumption for starch synthesis and other secondary metabolism.

However, the cycle of argumentation did not yet stop. The discovery of 14 subunits III in the ring structure of the CF_0 of the ATP synthase (Seelert et al. 2000; Scheuring et al. 2001; Seelert et al. 2003) raised the question of whether the actual requirement could be $14H^+$/3ATP. In this case the proton deficiency of at least 17% still must be covered either by the H^+-coupled cyclic electron flow around PS I or by linear electron flow to alternative acceptors other than CO_2. Despite the strong structural argument, the work of our group showed neither CET nor LET to alternative acceptors is existing at such a rate that could cover the 17% deficiency in the H^+ budget (Ref. III Laisk et al, 2007). We hope that the story is finished by the recent work of (Steigmiller et al. 2008), who determined the stoichiometry of H^+/ATP by chemiosmotic measurements of liposome-trapped ATPases. The calculations based on thermodynamics clearly indicate that $H^+/ATP = 4.0 \pm 0.2$ for the spinach chloroplast.

Presently, most investigators share the view that CET is H^+-coupled and its role is to cover the deficiency in ATP synthesis and to build up a regulatory proton gradient. Nevertheless, despite the long history of studies, evidence about the actual importance of cyclic photophosphorylation in plant leaves is still controversial and needs further investigation (Heber et al. 1995; Cruz et al. 2005).

2.5.4. Putative pathway of CET

Different mechanisms of CET have been proposed (Breyton et al. 2006): (i) the restricted diffusion model, according to which CET is concentrated around PSI located in non-apressed thylakoid membranes; (ii) the supercomplex model, assuming CET can occur in tightly bound PS I-Cyt b6f supercomplexes; (iii) the FNR- model, according to which PS I containing bound FNR functions in LET, but PS I without bound FNR reduces Fd, facilitating CET and (iv) the competition model, based on kinetic competition between LET and CET pathways.

In order to be efficient in proton translocation and ATP synthesis, the CET pathway must transfer electrons from a PSI acceptor side carrier, most likely Fd, to oxidized PQ. It has been shown that Fd and FNR have the central role in CET as electron carriers. The so reduced PQH_2 is then oxidized by the Q-cycle, coupled with H^+ transfer and ATP synthesis. At first a hypothetical enzyme Fd/PQ reductase was postulated (Bendall and Manasse 1995), but this enzyme has never been found. Instead, the most probable route for CET is assumed to be from the acceptor side of PSI, via Fd and FNR through the Cyt b_6f complex to the PQ pool (Joliot et al. 2004; Johnson 2005). The observation that FNR binds tightly to the Cyt b_6f complex providing a possible Fd binding site on this complex is also reported (Zhang et al. 2001). The proposed pathway assumes that Fd donates electrons to the high-potential Cyt b_H heme of the Cyt b_6f complex either directly or via Cyt c, and further to PQ at the Q_n pocket. This way the cycling electrons enter the Q-cycle and are believed to be coupled with H^+ transport. At the Q_p pocket two electrons are transferred from PQH_2, one to the Cyt b chain and the other to the soluble PC via the high potential chain (Rieske FeS and Cyt f) and protons are released into lumen side.

Such ATP-synthesizing CET is thought to function mainly around PSI located in the stroma-exposed thylakoids (Albertsson 1995). In these thylakoids PSII is almost absent, therefore, PSII does not compete with CET for PQ reduction. The acidification of thylakoid lumen generated by CET is assumed to be important for the production of ATP, but also for the induction of nonphotochemical quenching – the thermal dissipation of excitation from the PS II antenna (Johnson 2005; Lintala et al. 2007). For this reason it is widely believed that CET is essential in stress conditions, e.g. in case of water deficit (Arnon et al. 1958).

2.6. Measurement of cyclic electron transport

CET is believed to be relatively slow compared with LET. As told above, it is faster in light saturation and in stress situations, where electron acceptors are in deficit or the electron carriers are inactivated metabolically or genetically. CET

is also relatively high when LET is restricted, like under low CO_2 and O_2 concentrations.

The correct measurement of CET, however, has been a difficult experimental task, because CET is only a small part of the total ETR through PSI and it can only be measured as a difference, e.g. $J_{Cyc} = J_I - J_{II}$ (here J denotes ETR and subscripts specify the place CET is measured). ETR through PSII, J_{II} can be measured conveniently using Chl fluorescence [$J_{II} = a_{II}*I*(F_m - F)/F_m$], however, ETR through PSI, J_I, is difficult to measure. In contrast to PSII, the antenna chlorophylls of PSI do not emit variable fluorescence that would conveniently indicate PSI ETR. Because of these difficulties of measurement CET has often been evaluated indirectly, mainly on the basis of its expected consequences:

1) ATP synthesis (Arnon et al. 1956; Hosler and Yocum 1985; Hosler and Yocum 1987);
2) increased light energy conservation in photoacoustic measurements (Herbert et al. 1990; Havaux 1992; Cha and Mauzerall 1992);
3) increased membrane potential (electrochromic shift) (Hope and Morland 1980);
4) measuring postillumination rereduction rate of $P700^+$ (Harbinson and Hedley 1989);
5) inhibiting CET (Tagawa et al. 1963; Joet et al. 2001)
6) enhanced non-photochemical quenching (Yamamoto et al. 2006) and a small post-illumination transient peak in chlorophyll fluorescence have also been interpreted to indicate CET (Munekage et al. 2004);

2.6.1. Increased ATP synthesis

Reliable direct measurements of ATP synthesis can be carried out only *in vitro*. These measurements have demonstrated that a cyclic process really leads to ATP synthesis (Bendall et al. 1995; Allen 2003). However, CET is often difficult to distinguish from the pseudo-cyclic process that also is able to generate ATP, in which electrons are transferred from water to oxygen via the acceptor side of PSI (Badger 1985).

2.6.2. Photoacoustic spectroscopy

This technique is based on the quantification of the conversion of absorbed light energy to heat. The sample (photosynthetic bacteria, algae, infiltrated leaf) is placed in a photoacoustic cell which is closed or separated with gas-permeable membrane (Buschmann et al. 1984). If the sample is excited by absorption of modulated light (normally between 2 Hz – 2 kHz), heat pulses are generated with the same modulation frequency as that of the incident excitation light

(Herbert et al. 1990; Fork and Herbert 1991). These heat pulses create pressure changes in the thin gas phase above the sample and can thus be detected by a sensitive microphone as an acoustic signal. The absorbed light energy is divided into three parts: fluorescence, heat and photosynthesis. If light energy is used for chemical energy storage as a result of photochemistry, heat dissipation decreases, resulting in a decreased photoacoustic signal. Many measurements have led to the conclusion that, whilst cyanobacteria, green algae, and C_4 plants are capable of energy storage in far-red light (exciting only PSI, thus, potentially causing CET), C_3 plants are not (Herbert et al. 1990). Photoacoustics do not provide a specific measure of CET, but the energy occlusion may be interpreted as CET causing ATP formation. The advantage of photoacoustic measurements is that oxygen reduction should be detectable with modulated light/pressure change (Buschmann et al. 1984; Havaux 1992; Cha et al. 1992).

2.6.3. Estimation CET by membrane potential and change of Cyt f redox state

A membrane potential change is associated with the movement of protons and transport of electrons. The variations in the local dielectric environment influence protein structure, which causes changes of protein-bound pigment molecule spectra. Therefore the change of the membrane potential is measured as the electrochromic shift (ECS) of pigments, especially chlorophyll b and carotenoids, which induces significant absorption changes around 515 – 520 nm (Chow and Hope 1998; Sacksteder et al. 2000). Experimentally, the shift of electric field and the shift of pH have been found to be roughly parallel, which means that pH change should be approximately proportional to ECS (Cruz et al. 2001; Kanazawa and Kramer 2002). Even though ECS is quite well investigated in different conditions, interpretation of its size, shape and kinetics is still incoherent. When a sample is exposed to single turnover light flashes, multiple processes are present in the same time: 1) charge separation at the reaction centres; 2) transfer of electrons to secondary acceptors; 3) filling holes at P680 and P700; 4) uptake of protons at the stroma side; 5) release of protons to the lumen side; 6) proton delocalization through ATPase. Therefore, fast and slow components of transition are separated with the aim to discriminate between different processes. The fast component is considered to be charge separation or primary electron movement and the slow component is the electrogenic effect of electron or proton transfers across the Cyt b_6f complex and ATPase (Hope et al. 1980). Another disadvantage of usage of the 520 nm signal is some overlapping of spectral bands caused by ECS and by redox changes of cytochromes f (554 nm) and b and plastocyanin. The contributions by P700 and Cyt f could be distinguished when changes were measured as the difference at 518 – 485 nm (Joliot et al. 2004). To be more precise, additional measurements around 554, 564 and 575 nm are performed and the signals deconvoluted (Chow

et al. 1998; Kramer and Sacksteder 1998; Joliot and Joliot 2001; Finazzi et al. 2005; Golding et al. 2005). The rate of CET has been determined under saturating light excitation by measuring the postillumination rate of decay of the membrane potential or re-reduction rate of Cyt f (Joliot and Joliot 2002; Joliot and Joliot 2006). Inhibitors (DBMIB, DCMU, lincomycin, antimycin A) have also been used in order to separate changes in ECS caused by LET and CET (Patel et al. 1986; Chow et al. 1998; Chow and Hope 2004b).

2.6.4. $P700^+$ measurement

When P700, the reaction centre chlorophyll in PSI, is oxidized to $P700^+$ a strong bleaching occurs at 700 nm, but in intact leaves the decrease in absorbance at 700 nm is masked by the strongly overlapping dynamic chlorophyll fluorescence signal. However, the P700 oxidation can also be monitored as wide absorption increase around 800 – 830 nm. This far-red light is not actinic and is free of fluorescence, therefore, it is possible to apply high measuring beam intensities without disturbing the photosynthetic machinery.

Such measurements of P700 redox state can provide direct information on the total electron transport through PSI reaction centre. The experimental conditions must be specifically designed and data must be carefully interpreted in order to provide information on CET. Another problem is that the 810 nm transmission signal is not a specific indicator of $P700^+$, but three PSI-related components – PC^+, $P700^+$ and Fd^- – can contribute to the signal, and those optical effects are not proportional to $P700^+$ (Harbinson et al. 1989; Klughammer and Schreiber 1991; Kobayashi and Heber 1994; Schansker et al. 2003). The contribution of PC^+ is approximately 35% of the total absorbance at 810 nm and that of Fd^- may be up to 10% under strongly reducing conditions. Since these redox changes occur simultaneously but not proportionally, methods for the deconvolution of the 810 nm signal are needed for the correct interpretation of measurements. Additional differential measurements at 860–870 nm have been therefore performed and the two signals have been deconvoluted in redox states of PC and P700 (Joliot and Joliot 1984; Kirchhoff et al. 2004; Chow and Hope 2004a; Cassan et al. 2005; Golding et al. 2005; Joliot et al. 2006; Fan et al. 2007; Lintala et al. 2007). However, since there are three optical contributors, the dual-wavelength deconvolution is still insufficient. Alternatively, a deconvolution method based on redox equilibrium model of P700, PC and (Cyt f + FeS) has been applied (Oja et al. 2003).

2.6.5. Inhibition of CET

One way to evaluate the role of CET is to inhibit it and look at the resulting changes in photosynthesis. The cyclic electron transfer reactions around PSI have been reported to be inhibited by antimycin A (Tagawa et al. 1963). However, the mechanism of this inhibition is not clear. This opinion has been questioned by experiments on intact leaves (Joėt et al. 2002; Joliot et al. 2004). The existence of an antimycin A-insensitive type of CET was also proposed in C_3 plants from experiments performed *in vitro* (Hosler et al. 1987; Scheller 1996). The effect of antimycin A is based on its binding at the Q_n pocket of the Cyt b_6f complex, leading to the suggestion that this site is involved in electron flow. On the other hand, 2-heptyl-4-hydroxy-quinoline N-oxide (HQNO), an inhibitor binding at the Q_h pocket, did not affect CET (Rich et al. 1991; Johnson 2005). Anyway, if antimycin A binds at the Q_n pocket, it also inhibits the Q-cycle, thus making it difficult to interpret the changes observed in photosynthesis. It also has been reported that CET is sensitive to 3-(3,4-dichlorophenyl)-1,1-dimethyl urea (DCMU) and methylviologen (MV), suggesting an important role of so-called "redox poising" by the inhibition of PSII linear flow (Joliot et al. 2004; Fan et al. 2007). The "redox poising" is more important when O_2 and NO_2^- is present in reaction mixture (Bendall et al. 1995).

2.6.6. An alternative CET pathway via chloroplast NADPH oxidoreductase

In CET electrons can be also recycled via the type I NAD(P)H dehydrogenase (NDH) complex to PQ and subsequently to the Cyt b_6f complex. The latter route is known to be involved in the dark reduction of the PQ pool (Sazanov et al. 1998; Joet et al. 2001). A gene coding an NDH which is similar to the mitochondrial complex I has been identified in the genome of higher plants. However, biochemical analyses have shown that the concentration of this enzyme is much lower (<1%) than that of components of the photosynthetic electron transfer chain. If the concentration of NDH is a few percent of that of PSI, this enzyme could not stake to CET: its operation rate must be $10^3 – 10^4$ s^{-1} to sustain a rate of CET of 10 – 100 s^{-1} (Joliot et al. 2004).

2.6.7. CET connections with other alternative pathways

Reduced Fd, which is considered to be the main carrier in CET pathway, donates also electrons for nitrogen and sulphur reduction by corresponding enzymes, or to reduce sulphydryl groups of redox-activated enzymes (Neuhaus et al. 2000). Though the focus of this dissertation is on CET, a few words still

have to be said about alternative electron acceptors, because their importance considerably increases after CET will be significantly disqualified as a proton transporter as a result of this dissertation work. In photosynthesis the "alternative" electron acceptors are those other than PGA, mainly dioxygen (the Mehler reaction), nitrite and oxaloacetate, all of which have shown to be reduced by the photosynthetic electron flow at the acceptor side of PS I. Importantly, in order to improve the ATP/NADPH budget for photosynthesis, the further metabolism of compounds formed as the result of these alternative reductions must consume less ATP than the metabolism of sugar phosphates (or consume none at all). As a result, electron flow to the alternative acceptors will produce some extra ATP that can cover a deficit in the ATP budget of carbon reduction.

There is not much information available about the actual rates of these alternative reductions. The rate of the Mehler type O_2 reduction followed by the ascorbate peroxidase cycle (a cyclic process beginning with water oxidation and ending with O_2 reduction to water, or the "water–water cycle"), may be rather fast when the carbon reduction–oxidation cycle is an inefficient acceptor, e.g. during the dark–light induction or during CO_2-limited photosynthesis (Asada 2006). During fast photosynthesis only rates of <10% of the linear electron flow have been detected in C_3 and C_4 plants (Badger et al. 2000; Heber 2002; Siebke et al. 2003) (Ref III. Laisk et al, 2007).

Nitrite reduction (Joy and Hageman 1966) has been also suggested to be an important alternative electron sink balancing the ATP/NADPH stoichiometry during photosynthesis. Rates of nitrite reduction of up to 10% of LET have been suggested (Noctor and Foyer 1998), however, quantitative experimental evidence is vague (Baysdorfer and Robinson 1985; Robinson 1986; Robinson 1990).

Another pathway transporting excess reducing power out of chloroplasts is the "malate valve" (Scheibe 1987; Backhausen et al. 1994). In chloroplasts, malate dehydrogenase (MDH) reduces oxaloacetate (OA) to malate at the expense of NADPH generated in photosynthesis. The malate/OA transporter shuttles the substrates between the cytosol and the chloroplast. In the cytosol, malate is oxidized to OA, reducing the cytosolic NAD system, or is further metabolized in mitochondria.

3. AIM OF THE STUDY

As explained above, 3ATP/2NADPH is the strict stoichiometry of assimilatory-reducing power required for the conversion of CO_2 to sugars in photosynthesis. But for over half a century the photosynthetic ATP/NADPH production ratio has been a subject of debate. The amount of consumed NADPH is defined by the rate of carbon reduction, but any deficit of ATP during the same process is believed to be corrected mainly by H^+-coupled cycling of electrons around PSI, commonly referred to as cyclic photophosphorylation. The correct measurement of cyclic electron transport (CET) has been a difficult experimental task, first, because CET is only a small part of the total PS I electron transport rate (ETR) and, second, in contrast to PSII, the antenna chlorophylls of PS I do not emit variable fluorescence that would conveniently indicate PS I ETR. The aim of this work was to carry out methodically most correct measurements of CET in intact leaves and look whether the results confirm the role of CET as an additional ATP producer by cyclic photophosphorylation or the results contradict to this view. The results showed that CET is very fast during light-saturated photosynthesis, but is undetectably slow during light-limited photosynthesis. The kinetic behaviour of CET – especially its fast rate under photosynthetically inactive far-red light – is not compatible with the role of CET as the source of additional ATP. To explain the result, an electron transport pathway allowing for proton-uncoupled CET is proposed.

4. MATERIAL AND METHODS

4.1. Plants

The specificity of this work is in the object of measurements – experiments were carried out on intact leaves with the aim to understand the functioning of a completely intact photosynthetic system. In most cases the object was sunflower (*Helianthus annuus* L.) – a plant with a relatively powerful C_3 photosynthetic machinery. Transgenic potato (*Solanum tuberosum* L.) with over- and underexpressed levels of malate dehydrogenase (MDH) was used in studies of alternative electron transport routes.

Plants were grown in laboratory in growth chambers (AR-95HIL, Percival, from CLF Plant Climatics GmbH, Emersacker, Germany) at a PFD of 450 μmol quanta m^{-2} s^{-1}, 14/10 h day/night cycle, 25/20º C temperature, and RH of 70%. Full-grown leaves attached to the plant were used in measurements.

4.2. Rates through different complexes of the electron transport chain

Rate through different parts of the photosynthetic electron transport chain was measured using different methods: ETR through PSII, J_{II}, was calculated either from chlorophyll fluorescence parameters or from O_2 evolution measurements; ETR through PSI, J_I, was found from optical transmittance measurements indicating redox changes of PSI donor side electron carriers PC and P700; ETR for carbon reduction, J_C, was calculated from net CO_2 uptake measurements considering the photosynthetic and photorespiratory components as determined by Rubisco kinetics. CET (denoted J_{Cyc}) was calculated as a difference between the measured ETR components.

There are several approaches to define J_{Cyc}. First, $J_{Cyc} = J_I - J_{II}$. This approach assumes all electrons passing through PSII (J_{II}) form LET that also passes through PSI. If PSI turns over faster than PSII the difference is J_{Cyc}. This approach neglects the possibility of electron cycling around PSII, which, however, is a significant component of PSII electron flow (Laisk et al. 2006). Due to PSII cycling, all electrons passing through PSII do not pass through PSI. Considering the PSII cycle, in (Ref. III) the CET rate was calculated as a difference between the rate through PSI and the rate of electrons leaving PSI, $J_{Cyc} = J_I - (J_C + J_{Alt})$, where J_{Alt} is electron flow to reduce alternative acceptors other than CO_2. Only if the PSII rate was very small (as under FRL in Ref. I and II) the PSII cycle was neglected, calculating $J_{Cyc} = J_I - J_{II}$. The reliability of conclusions is therefore based on the measurements of J_I and J_C (and J_{Alt}). However, it needs to be emphasized that crucial experiments were carried out under conditions were J_I was fast, but J_{II} and J_C were much slower (illumination

under far-red light, FRL) – an approach that significantly increased the reliability of the conclusions concerning CET (Ref I and II).

4.3. Measurement of PSI electron transport

The principle approach for the measurement of J_I was that of the "postillumination re-reduction". Under high-intensity actinic white light (or under FRL) the PSI donors P700, PC and Cyt f are at least partially oxidized, because PSI is excited very frequently, but electron arrival at PSI is rate-limited by the turnover of Cyt b_6f. After illumination is suddenly interrupted, electrons continue arriving (from the reduced PQH_2 pool) into the oxidized Cyt f^+, PC^+ and $P700^+$ at the same rate as previously in the light. Later the rate declines because $P700^+$, PC^+ and Cyt f^+ gradually become more reduced and PQH_2 becomes more oxidized. Thus, the initial post-illumination rate of reduction of $P700^+$, PC^+ and Cyt f^+ reflects the steady-state rate of PSI electron transport.

The PSI rate was measured this way using optical signals, characteristic to the reduction of these electron carriers. Either single wavelength measurements were carried out at 950 nm, complemented with the condition of redox equilibrium between Cyt f ↔ PC ↔ P700 to calculate the redox states of individual electron carriers, or dual wavelength measurements at 810 and 950 nm were applied to deconvolute the redox states of the electron carriers. The application of the redox equilibrium condition (proven in Ref. II) allowed us to avoid the optical interference by Fd^-, the third signal source not deconvoluted from the dual wavelength measurements. In solutions and suspensions it is a common practice to calculate the absolute amount of an optically active compound using its known optical absorption coefficient. However, leaves are optically disperse, the actual optical pathway of the measuring beam is longer than leaf thickness, dependent on leaf structure and its water status. Therefore, for the calculation of absolute amounts of the optically active compounds in leaves the optical measurements must be calibrated individually for each leaf. The corresponding procedure is called "oxidative titration by far-red light" (the term is based on the analogy with chemical titration, since the change of the titratable component is induced by the applied FRL) (Oja et al. 2003).

4.4. Oxidative titration of PSI donors by far-red light

The essence of the procedure is in the time course of the optical signal during (slow) cumulative oxidation of the PSI donor side carriers by FRL. The principle of the method is simple. In the dark, the high-potential PSI donors (P700 + PC + Cyt f) are all reduced. When FRL is applied, first Cyt f, then PC and finally P700 are being oxidized, as defined by the progressively increasing E_m values of these compounds. The same time course of the optical signal is

also calculated from the model of redox equilibrium (undoubtedly valid during the slow oxidation). The parameters of the model – the pools of P700, PC and Cyt f – are varied until the best fit between the measured and calculated time course is achieved. The equilibrium constant between PC and P700 is independently found from the dual wavelength measurements, while that between Cyt f and PC is calculated from the difference of E_m.

The quantum efficiency of electron transport through PSI with reduced donor and oxidized acceptor is about 95%. There is also some PSII excitation under FRL (about 6%, Ref. II). However, the most interfering with the FRL titration is CET induced by FRL, due to which the donor side carriers are continuously re-reduced during the titration (oxidation) procedure. In order to avoid complications due to CET (and also due to the PSII electron transport), only the very first few milliseconds of the time course were used for the calculations. In order to cover the whole redox span, the PSI donors were maximum oxidized under steady-state FRL, then FRL was turned off and the carriers were let to be re-reduced in the dark to different extent, before the FRL was turned on again and the very initial rate of optical signal change was recorded. An example of the recordings and of the model fitting is shown in Fig. 3 of Paper I. For this example the best-fit pools were P700 = 1.41 μmol m^{-2} , and there were 3.3 PC/P700 and 0.8 Cyt f/P700. The per electron sensitivity of the optical signal is highly nonlinear in the 810 nm spectral range, being most sensitive when $P700^+$ is being oxidized, less sensitive when PC^+ is being oxidized and no signal is generated when only Cyt f is being oxidized. At 950 nm the per electron sensitivity is more uniform over the whole redox span (Fig. 10). Though the total signal was smaller, the 950 nm wavelength was used in many measurements in order to avoid the interference by Fd^- (Fd^- gives practically no signal at this wavelength).

Such an oxidative titration procedure of PSI donor side pools was checked against the reductive titration procedure (Oja et al. 2004). In this procedure the PSI donor pools are calibrated against O_2 evolution measurements. During a steady state under FRL (interphotosystem carriers oxidized) the leaf is illuminated by a single-turnover flash. The number of electrons generated by the flash is calculated as four times the corresponding O_2 evolution. After a few ms these electrons arrive at PSI, causing some (incomplete) reduction of the donor side carriers. The PSI donor side pools are found from the extent to which they are reduced by the known number of PSII electrons.

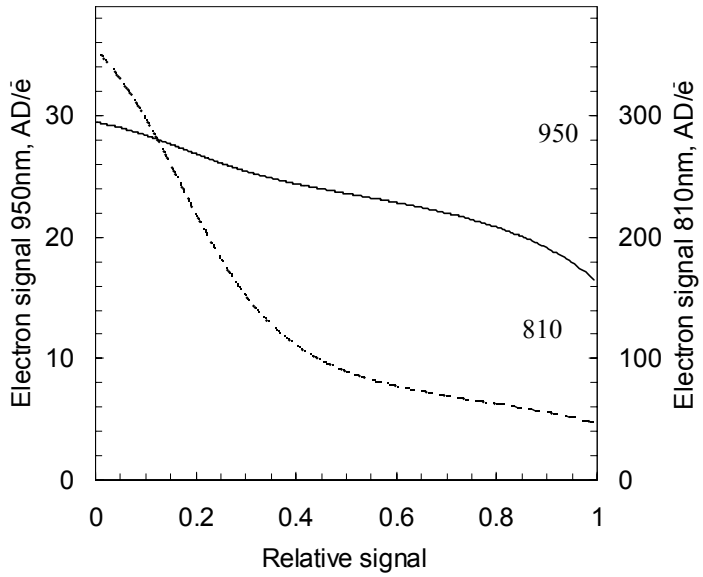

Figure 10. Comparison of 810 nm and 950 nm signal sensitivities per e^-. Zero of the signal corresponds to complete oxidation, 1.0 to reduction.

4.5. Electron transport rate through PSII

The electron transport rate through PSII (J_{II}) was calculated from Chl fluorescence as follows (Genty et al. 1989):

$$J_{II} = \alpha I a_{II} \frac{F_m - F}{F_m} ,$$

where F_m is maximum pulse-saturated fluorescence yield, F is the steady-state yield, I is incident photon flux density, α is absorption coefficient and a_{II} is the relative optical cross-section of PSII antenna. The fluorescence parameters were measured with the PAM 101 (H. Walz, Effeltrich, Germany) fluorometer, incident light intensity was measured with the quantum sensor LI-190SB (LiCor, Lincoln, NE), leaf optical absorptance was measured in an integrating sphere with the spectroradiometer PC-2000 (Ocean Optics, Linn FL) and the optical cross-section of PSII was measured from the maximum quantum yield of gross CO_2 fixation corrected for the fluorescence-indicated losses (Laisk et al. 2002).

4.6. Electron transport rate for carbon reduction

Electron transport consumed for carbon reduction was calculated from the measured rate of net CO_2 fixation, considering its partitioning into the photosynthetic CO_2 uptake, photorespiratory CO_2 evolution and dark respiratory CO_2 evolution in the light. First, dark respiratory CO_2 evolution, R_K was determined dependent on light intensity, such that the quantum yield of PSII, J_{II} calculated from fluorescence, would stay constant at the lowest light intensities below and slightly above the light compensation point (Laisk et al. 2002). Usually at low light intensities R_K decreased by 30–40% compared to the value measured in the dark. After R_K was subtracted, the remaining CO_2 exchange was partitioned between photosynthesis and photorespiration according to the kinetic properties of Rubisco dependent on the intrachloroplast CO_2 concentration C_C according to the equation (Laisk et al. 2002):

$$J_C = 4(A_C + R_K)\frac{2K_sC_c + 2O_c}{2K_sC_c - O_c},$$

where A_C is the measured net rate of CO_2 assimilation, R_K is the rate of Krebs cycle respiration in the light, K_S is the CO_2/O_2 specificity factor of Rubisco, and C_C and O_C are the dissolved CO_2 and O_2 concentrations (mM) at the carboxylation site.

5. RESULTS AND DISCUSSION

5.1. PSI Cyclic Electron Transport Under Far-Red Light

5.1.1. CET in dark-adapted leaves and inactivation of FNR

As explained above, CET is defined as a difference between PSI ETR (J_I) and either PSII ETR (J_{II}) or ETR for carbon reduction (J_C). Usually under normal photosynthetic conditions under white light the difference characterizing CET is rather small, about 10 to 30% of the total PSI ETR. The idea of experiments described in this section was to measure CET under conditions where J_{II} and J_C are slow, but PSI ETR J_I is relatively fast. Such conditions exist under illumination with FRL (720 nm), dominantly exciting PSI (94%) and only 6% of the quanta exciting PSII. The PSI ETR J_I was measured as the initial rate of electron arrival into the PSI donors after FRL was interrupted.

In these experiments unexpected responses of sunflower leaves were recorded when FRL was turned on again after darkening for different time intervals. The oxidation of the PSI donors was fast (within 0.5 s, as expected) when the preceding dark exposure was brief (15 s to one minute), but the oxidation was slow and incomplete after longer dark exposures (Paper I, Fig. 4). When the applied FRL was turned off again after 1 s exposure, the rate of the post-FRL re-reduction was 2 e^- s^{-1} per PSI after short darkening, but increased to 13 e^- s^{-1} per PSI after 500 s of darkening. This showed that the inability of FRL to oxidize the PSI donors was caused by fast CET. When FRL was turned on after short darkening the maximum of five electrons occupying the PSI donors (1e^- in P700, 3 e^- in PC and 1 e^- in Cyt f as determined by the oxidative titration) were rapidly carried through PSI by FRL and further transported through Fd and ferredoxin-NADP reductase (FNR). Only 2 e^- s^{-1} per PSI returned via CET. After long darkening most electrons could not proceed through the pathway towards NADP, but were forced to return to the PSI donor side at the maximum rate of 10 e^- s^{-1} per PSI. This suggested that the linear electron transport pathway leading to NADP, most likely ferredoxin-NADP reductase, becomes inhibited during longer dark exposures exceeding 2 minutes.

The re-activation of FNR in the light was studied by recording the time course of the oxidation of the PSI donors under strong FRL. After relatively brief dark exposures the following oxidation process was fast and there was only a small secondary reduction peak observable. With increasing the length of the dark exposure the temporary reduction peak increased, but retrieved within 3 s (Paper I, Fig. 7). This shows that the strong FRL rapidly transferred all the 5 e^- from the donor side to the acceptor side carriers involving Fd and probably the flavin of FNR. However, the continuing PSII electron transport under FRL

(6% of the FRL quanta excited PSII) produced additional electrons that no more could be accommodated on the available acceptor side carriers, but remained on the donor side because electron transport through PSI was blocked. Such a kinetic nature of the transient was evident when the experiment was repeated with a low-intensity FRL; then the re-reduction peak developed slowly even after the longest dark intervals.

It is noteworthy that the inhibition of FNR did not inhibit CET in these experiments, but, to the contrary, enhanced it. The CET rate proceeded through the maximum simultaneously with the maximum reduction of the electron carriers (Paper I, Fig. 8). It means that FNR, at least its light/dark-regulated component, is not involved in the CET pathway. When FNR is inhibited, more electrons are directed into the CET pathway.

5.1.2. Intrinsic maximum of CET

The above experiments showed that CET increased when linear electron flow from PSII to $NADP^+$ was restricted by dark-inactivation of FNR. Most experiments of Paper I were carried out with a low-power FRL source, therefore, the recorded maximum CET rate of 10–15 $e^- s^{-1}$ per PSI could be not the intrinsic maximum, but most likely was light-limited by the low FRL intensity. Further kinetic studies of CET were undertaken in Paper II with an aim to find the intrinsic limitations for CET. For this the FRL source was elaborated for the maximum incident FRL of 1200 μmol quanta $m^{-2} s^{-1}$.

In Paper I the maximum CET was obtained when FNR was dark-inactivated, but this state lasted only for a few seconds, making the studies of the intrinsic maximum of CET experimentally difficult. In Paper II, instead of the dark inactivation of FNR, CET was poised for its maximum rate by suitably limiting the availability of terminal electron acceptors CO_2 and O_2. These measurements of PSI ETR were based on optical signals generated by $P700^+$ and PC^+ in two wavelengths, of 950 and 810 nm. This experimental approach made the deconvolution of the redox states of P700 and PC directly from the optical measurements possible. These deconvolutions showed that the redox ratio $P700/P700^+$ advanced proportionally with, but 35 times faster than, the redox ratio PC/PC^+. This is a clear demonstration that the redox equilibrium is present among the PSI donor side electron carriers P700 ↔ PC ↔ Cyt f during the post-FRL re-reduction transient. The value of the equilibrium constant of 35 corresponds to the difference of midpoint redox potentials of P700 and PC of 90 mV.

CET was measured in sunflower leaves exposed to high-intensity FRL (>400 μmol quanta $m^{-2} s^{-1}$). O_2 was eliminated from the gas (20 μmol O_2 per mol gas was present), in order to completely suppress photorespiration and to make the measurement of PSII ETR possible by using the O_2 evolution measurements with a zirconium cell O_2 analyzer. The linear ETR, caused by

PSII excitation by the applied FRL, was rate-limited by decreasing CO_2 concentration stepwise from 360 to 0 μmol mol^{-1} with the aim to induce CET by creating the deficit of acceptors for LET. During such a steady-state situation, the FRL was turned off and the post-FRL transmittance changes at 950 and 810 nm were recorded (Paper II, Fig 3 A, B). The 950 and 810 nm signals were scaled between the full reduction (in the dark) and full oxidation (saturation pulse superimposed on FRL) levels and were deconvoluted into the absolute number of electrons (μmol m^{-2} or e^- per PSI) in all PSI donors, P700 + PC + Cyt f (Paper II, Fig. 7). At high CO_2 concentrations FRL completely oxidized PC and only a small part of the P700 pool remained reduced (0.2 e^- per PS I in the donor side carriers). This reduced fraction of P700 supported transport through PSI of electrons generated by PSII plus electrons cycling around PSI under FRL. As CO_2 concentration decreased, the steady-state content of electrons on the PSI donor side increased. Since the excitation rate was constant, the progressive increase in steady-state reduction of P700 indicated faster CET as the CO_2 concentration decreased.

The best indicator of the PSI ETR is the initial slope of the post FRL transients. Figure 8 of Paper II shows the total electron flow rate through PSI as calculated from the initial slope of each post-FRL trace. The rate was slow (about 30 μmol e^- m^{-2} s^{-1}) when CO_2 did not limit LET, but it increased as CO_2 concentration decreased, approaching a peak of 75 μmol e^- m^{-2} s^{-1} at the CO_2 level of 12 μmol mol^{-1} (PSI content = 2.2 μmol m^{-2} in the example leaf, but these absolute values varied between leaves dependent on stomatal opening and probably the levels of intermediates in the carbon reduction cycle). Further decreases in CO_2 concentration decreased the total PSI electron flow again due to the overreduction of the PSI acceptor side (closure of PSI centres). While the PSI ETR was fast, the maximum PSII ETR was only 14 μmol e^- m^{-2} s^{-1} and this rate decreased with decreasing CO_2 concentration to about 5 μmol e^- m^{-2} s^{-1}, as indicated by simultaneous O_2 evolution measurements.

The CET rate was calculated as the difference between total PSI flow and PSII flow: $J_{Cyc} = J_I - J_{II}$ (considering that the PSII cycle could not be fast under FRL because of the slow PSII excitation). CET was about as fast as LET at higher CO_2 concentrations (about 15 μmol e^- m^{-2} s^{-1} each), but CET rapidly increased as CO_2 became limiting for LET, approaching a maximum of 70 μmol e^- m^{-2} s^{-1} at 12 μmol CO_2 mol^{-1}, whilst LET was limited to only 5 μmol e^- m^{-2} s^{-1}. As noted above, the maximum CET rate varied dependent probably on the concentration of photosynthesis products. In the 13 examined leaves the average CET rate was 30, extending from 15 to 60 s^{-1} per PSI. This value is characteristic for the intrinsic maximum of CET at 22 ºC, which was the measurement temperature.

5.1.3. Donor and acceptor pools of cycling electrons

The kinetic data of Fig. 7, Paper II enabled one to estimate the donor and acceptor pools involved in CET around PSI. The idea is based on the analysis of not only the initial slope of the post-FRL curve, but of the running slope over the whole curve. The decreasing running slope indicates the decreasing rate of electron arrival. By plotting the slope as a function of the number of electrons transferred (the ordinate of Fig. 7, Paper II) makes it clear how PSI ETR decreases as a function of arrival of electrons into the donor pool (Cyt f + PC + P700).

At higher CO_2 concentrations the initial number of donor-side electrons was small, the initial PSI ETR was slow and further it rapidly decreased with the transfer to the donor side of 0.4–0.6 μmol e^- m^{-2} (Fig. 9, Paper II). This shows that under non-limiting CO_2 concentrations there were less than 1 e^- per PSI altogether in the pool of PQH supporting LET plus in the pool of Fd supporting CET. With decreasing CO_2 concentration the initial number of donor side-electrons and the initial ETR under FRL increased. This increase was caused by increasing CET, because PSII flow decreased with CO_2. In the leaf analyzed for the pools the maximum initial rate of 57 μmol e^- m^{-2} s^{-1} was observed at 40 μmol CO_2 mol^{-1}, when the upstream donor pool of CET contributed an additional 3.8 μmol e^- m^{-2} during the post-FRL phase. At CO_2 concentrations below 40 μmol mol^{-1} the upstream CET donor pool continued to increase, but then ETR to PSI decreased due to limitation by the number of electron vacancies on the PS I donor side (overreduction of the chain). The slopes of the traces in Fig. 9, Paper II represent first-order rate constants, where the initial slope of about 30 s^{-1} characterizes the rate constant for electron transfer from an upstream CET donor (possibly Fd^-) to the donor side.

In order to identify the possible rate-limiting acceptor of CET on the PS I donor side, electron transfer rate during the post-FRL transient was plotted against the fraction of either $P700^+$ (Paper II, Fig. 10A), PC^+ (not shown) or Cyt f^+ (Paper II, Fig. 10B) as deconvoluted from the dual wavelength plus redox equilibrium analysis. The rationale was to identify a carrier displaying about first order kinetics. The kinetic curves of PSI ETR versus Cyt f^+ (Paper II Fig. 10B) showed no proportionality at higher CO_2 concentrations, but at low CO_2 concentrations (10, and 20 μmol CO_2 mol^{-1}) a sustained proportional relationship was evident between ETR and the pool of oxidized Cyt f. This analysis shows that the rate-limiting step in CET resides closer to Cyt f^+ than to $P700^+$ on the PSI donor side.

5.1.4. Quantum efficiency of PSI during electron cycling

The quantum efficiency of PSI was investigated by varying PSI ETR in two ways. First, in light response measurements the incident FRL intensity was increased from 10 to 1200 μmol quanta m^{-2} s^{-1} at a constant CO_2 concentration of 360 μmol mol^{-1}. Second, in CO_2 response measurements under the maximum FRL, P700 became more reduced as CO_2 concentration decreased (Paper II, Fig. 7). PSI ETR is plotted against the FRL quantum flux rate exciting reduced P700 for the light response and CO_2 response measurements in Fig. 7 of Paper II. At low FRL values PSI ETR was very slow and the quantum yield of PSI with reduced P700 was only slightly less than 1.0 (as also shown on Fig. 9 of Paper I). The quantum yields tended to decrease as soon as CET increased at limiting CO_2 concentrations. However, the loss of PSI quantum yield did not exceed 30%, indicating the portion of charge recombination in PSI. Such a relatively high quantum yield of PSI (>70%) supporting CET has important implications. It shows that about all PSI in the leaf were able to perform in cycle, questioning the model according to which PSI located in the stroma-exposed thylakoids are preferentially functioning in cycle, but PSI in the grana margins are carrying out linear electron transport (Albertsson 2001). The fact that PSI quantum efficiency little decreased in parallel with the increasing CET rate shows that electrons poising CET accumulate on a PSI acceptor side compound having insufficiently negative E_m value to block electron transport through PSI. This is in agreement with the notion that Fd may be the CET donor.

After illumination the induction of CET was very fast, e.g., its rate increased by three times during 100 ms after a xenon flash (Paper I, Fig. 6.). This fast activation shows that CET is directly redox-controlled. This also shows that CET is functioning not only around PSI located in the stroma thylakoids far from PSII, but around every PSI that can rapidly receive electrons from PSII.

5.1.5. Cyclic electron flow and proton gradient

In order to see whether CET helps to generate proton gradient and synthesize ATP the experimental conditions were chosen such where ATP consumption for CO_2 fixation was close to nil. The low CO_2 and O_2 concentrations limited LET to only 5 e^- s^{-1} per PSI (Paper II, Fig. 8, Leaf 1) at CO_2 concentration of 40 μmol mol^{-1}. This LET supported a CO_2 fixation rate of 1.25 CO_2 s^{-1} per PSI, requiring 3.75 ATP s^{-1} per PSI. Such a rate of ATP synthesis required, at most 17.5 H^+ s^{-1} per PS I (assuming the maximum of 4.66 H^+/ATP), from which 15 H^+ s^{-1} per PSI were translocated coupled to linear flow, leaving a potential deficit of only 2.5 H^+ s^{-1} per PSI to be translocated by CET. The actual CET rate of 30 e^- s^{-1} per PSI (Paper II, Fig. 8) was capable of translocating 60 H^+ s^{-1} per PSI assuming CET was coupled to H^+ translocation via the Q-cycle

($2H^+/e^-$). Thus, the H^+ translocation capacity of the measured CET rate by far exceeded the H^+ translocation rate needed to correct the maximum conceivable deficit in the H^+ budget.

In order to investigate the relationship between CET and proton gradient, maximum pulse-saturated chlorophyll fluorescence (F_m) was measured, assuming that non-photochemical quenching (NPQ) is a reliable (though nonlinear) indicator of low lumenal pH. The measurements showed F_m was indeed quenched in parallel with increasing CET as the CO_2 concentration was lowered (Paper II, Fig. 12). To test the possibility that not CET, but rate-limited LET was the actual reason for increasing NPQ, we repeated the experiment with weak green light instead of FRL. The green light intensity was chosen such that it excited PSII at the same rate as FRL (about 30–40 μmol quanta m^{-2} s^{-1}, based on O_2 evolution measurements), but PSI was excited about equally with PSII; excess PSI excitation was not available for any CET, not speaking about the extreme fast CET observed under FRL. Nevertheless, F_m was quenched under green light at low CO_2 concentrations even somewhat more than under FRL. Thus, further limitation of even a very slow light-limited LET by availability of electron acceptors causes the build-up of a proton gradient sufficient to induce NPQ.

The result shows that there is practically no passive (ATP-uncoupled) proton leak through the thylakoid membrane. Since even a minimal LET can build up NPQ, CET is unlikely to constitute a primary source of the proton gradient. A theoretical possibility still remains that some overflow-type channels short-circuit the fast proton flow as soon as the proton gradient exceeds the normal NPQ range, but this mechanism would assume a special type of regulation of ΔpH and electron flow, not yet observed.

5.2. Cyclic Electron Flow Under White Actinic Light

The experiments described above were carried out under FRL with the aim to boost CET and suppress LET – a condition convenient for the investigation of the kinetics of CET, but far from normal photosynthesis. The following experiments were carried out on potato leaves under white actinic light (WL), exciting both photosystems about equally and thus causing fast LET – the condition of normal photosynthesis. The potato plants were wild type and transgenic, with over- and underexpressed chloroplast malate dehydrogenase (MDH). The transgenic potato plants were chosen with the aim to investigate the potential role of the MDH-related alternative electron transport pathway for the adjustment of the ATP/NADPH budget during photosynthesis.

PSI electron transport was measured with the same method as under FRL – by recording the initial rate of 810 nm signal change after the illumination was suddenly interrupted. Dual wavelength measurements were not applied, but the redox states of the PSI donors P700, PC and Cyt f were calculated from the

redox equilibrium condition. While the characteristic time of the postillumination transient was 100–200 ms after the interruption of FRL, then in the experiments under WL the characteristic time of the postillumination transient was about 30 ms (Fig. 5, Paper III). The difference shows the significant contribution of LET generated by PSII. Since under the strong WL electron cycling around PSII was fast, CET was measured as the difference between PSI ETR and ETR for carbon reduction, $J_{Cyc} = J_I - J_C$. Though under WL (and no strict CO_2 limitation) the cyclic component makes up only 25 – 30% (47% in maximum) of J_C, the applied optical techniques were precise enough to produce stable results.

At low light intensities limiting photosynthesis CET was very slow (actually not detectable, $J_I = J_C$), but J_I increased over J_C as soon as light became saturating for photosynthesis (Fig. 3, Paper III). The observed maximum rate of CET was 60 μmol e^- m^{-2} s^{-1} or 40–50 e^- s^{-1} per PSI, whilst ETR for carbon reduction, J_C, was 150 μmol e^- m^{-2} s^{-1}. Importantly, when O_2 concentration was decreased from 21% to 2% and CO_2 concentration down to zero, the CET rate remained about the same as under normal air conditions, or it even slightly increased (Fig. 6, Paper III). This result clearly shows that CET rate is not related to the CO_2 reduction rate, but CET is an independent process activated as soon as photosynthesis becomes light-saturated. The presence of fast CET under WL in the absence of CO_2 reduction once again shows that CET cannot serve for additional ATP production, i.e. it cannot be obligatorily coupled with proton translocation. The most likely physiological function of the fast H^+-uncoupled CET is to dissipate excess light energy under high illumination and limited availability of electron acceptors.

5.3. Proposed Pathway Of Cyclic Electron Transport

The presence of fast CET in leaves under conditions where CO_2 reduction is practically absent is explainable by two mechanisms: 1) if CET is coupled with H^+ translocation then the protons translocated by CET must be recycled through a membrane leak uncoupled from ATP synthesis and 2) CET itself can be uncoupled from H^+ translocation. There is no information about such overflow-type well-controlled (absent when H^+ is limiting and very fast when H^+ is in excess for ATP synthesis) proton leak. The fact that proton gradient inducing NPQ can be built up under very low light confirms the absence of proton leaks through the thylakoid membrane. In order to explain these experimental facts a CET mechanism allowing for variable e^-/H^+ coupling, including also complete uncoupling, was proposed (Fig. 11). The mechanism is based essentially on the reversed pathway of the Q-cycle. The basic novelty of this scheme is the ΔpH-regulated competition between LET and CET on PSI donor side, resulting in bypass of the PQ pool by CET flow, so that the CET-associated electron flow is uncoupled from proton translocation.

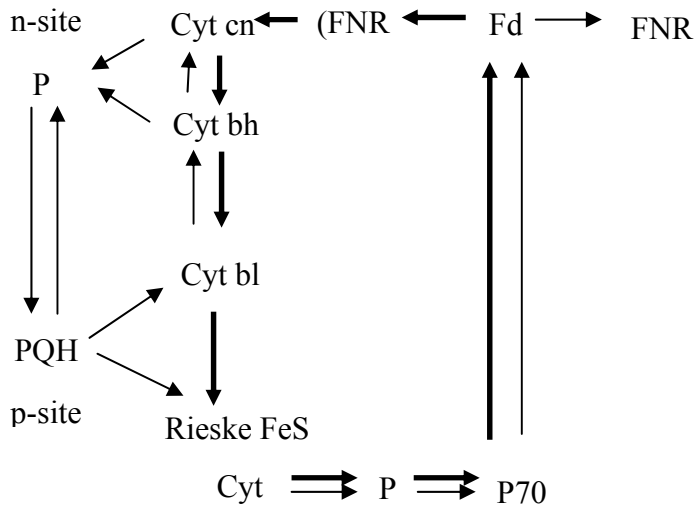

Figure 11. Proposed pathway of cyclic electron transport. Bold arrows – CET. Reactions of the linear pathway, competing with the cyclic pathway, are shown by thin arrows.

The scheme of Figure 11 is based mainly on (Baniulis et al. 2008), considering the possibility of double reduction of PQ simultaneously from Cyt b_h and Cyt c_n at the n-pocket of the Cyt b_6f complex (here the denotation of Baniulis et al. 2008 is used, n standing for the stromal or negative and p for the lumenal or positive side of the membrane). At low light intensities and high CO_2 and O_2 concentrations LET is favoured, because PQH_2 oxidation at the p-pocket of Cyt b_6f is not restricted by H^+ backpressure. Rieske FeS, Cyt b_l, Cyt b_h (and probably Cyt c_n) are rapidly reduced according to the Q-cycle mechanism and oxidized PQ is available for double reduction at the n-pocket inside the inter-monomer quinone exchange cavity (as reviewed by Baniulis et al. 2008). At light saturation, when low levels of CO_2 and O_2 limit RuBP carboxylation/ oxygenation, ATP consumption is limited, ADP depleted and protons accumulate in the thylakoid lumen. Then PQH_2 oxidation is slowed down by proton backpressure (Siggel 1974) leaving Rieske FeS and the hemes of the Cyt b_6f complex largely oxidized. Simultaneously, electrons accumulate on the PSI acceptor side carriers due to the limited availability of acceptors, creating favourable conditions for CET: on the PSI donor side high ΔpH limits the oxidation of PQH_2, while the limited availability of BPGA causes accumulation of electrons on the acceptor side, including in Fd.

How can CET be uncoupled in this model? CET is most active when ATP is in excess, i.e., when PQH_2 oxidation is down-regulated by high ΔpH, because otherwise the Rieske FeS and Cyt b carriers are reduced by electrons from PQH_2, out-competing CET. When PQH_2 is not oxidized, PQ is missing from the

inter-monomer quinone exchange cavity, explaining why PQ cannot be reduced at the p-pocket during CET. Thus, CET remains uncoupled from proton translocation, because no oxidized PQ is available for reduction at the n-pocket of PQ reduction inside the intermonomer quinone exchange cavity of the Cyt b_6f complexes. This model in principle proposes not totally uncoupled, but flexible e^-/H^+ coupling in CET dependent on redox conditions (poising) on PS I donor and acceptor sides. In intact systems like leaves, CET rate approaches the maximum under uncoupled conditions, but may be coupled when PSI acceptor side carriers become reduced under the conditions of low proton gradient.

The critical point of the scheme of Figure 11 is the assumption that Rieske FeS can be reduced by Cyt b_l when PQH_2 cannot be oxidized due to high H^+ backpressure (strong photosynthetic control). Presently available analyses focus on the mechanism of the bifurcated reaction of PQH_2 oxidation (Berry et al. 2000) in the state of absence of the photosynthetic control. In the case of fast CET PQH_2 cannot be oxidized at the p-pocket, either because of the strong H^+ counter pressure or because the hemes b_l and b_h are reduced by the CET pathway. There is little information how the oxidation of PQH_2 is prevented under such a strong photosynthetic control. The critical question is whether under this condition electrons can pass from Cyt b_l to Rieske FeS and further on to Cyt f? That is, if PQH_2 approaches the p-pocket but cannot be deprotonated, is electron exchange through the Cyt $b_l \leftrightarrow$ Rieske FeS link possible without net H^+ exchange? This work cannot answer these molecular-mechanistic questions, but it shows that such fast electron transport through Cyt b_6f complex does occur without the coupled oxidation of PQH_2.

6. CONCLUSIONS

6.1. This dissertation work has established the following experimental facts.

1. Cyclic electron transport around PSI (CET) is absent (or very slow) during light limitation, but fast during light saturation of photosynthesis; it remains fast when photosynthesis is strictly rate-limited by low CO_2 and O_2 concentrations.
2. CET is fast when PSI is excited by far-red light (FRL), but the slow linear electron flow (caused by PSII excitation by FRL) is rate-limited by the availability of electron acceptors, e.g. due to inactivation of ferredoxin-NADP reductase or by very low CO_2 and O_2 concentrations.
3. CET donor pool on PSI acceptor side contains up to 4 e^- per PSI that must become reduced in order to initiate CET.
4. CET acceptor on PSI donor side is not $P700^+$, but an electron carrier with more negative redox potential than P700, most likely Cyt f.
5. The kinetics of electron transfer from the CET donor to the CET acceptor are biphasic, the first electron transferred with the rate constant of 30 s^{-1}, but the following electrons transferred with the rate constant of 10 s^{-1}.

6.2. The established experimental facts are interpreted to mean the following (model) understandings

1. The absence of correlation between CET and photosynthetic rate suggests that CET is not always important to maintain the necessary ATP/NADPH stoichiometry during photosynthesis. Rather, under excess light CET is an energy-dissipating process protecting the photosynthetic machinery from the formation of reactive oxygen species under excess irradiation.
2. The fact that $P700^+$ is not an immediate CET acceptor rules out the possibility that the measured post-illumination electron flow from PSI acceptor to its donor side was charge recombination.
3. The following functional pathway of CET is suggested: Fd (or PSI-bound FeS e^- carriers) → FNR (?) → Cyt c_n → Cyt c_h → Cyt c_l → Rieske FeS → Cyt f → PC → P700 → (bound FeS) → Fd. The CET pathway is out competed by PQH_2 oxidation at the p-pocket of Cyt b_6f, but the CET pathway activates when PQH_2 oxidation is restricted in the presence of high transthylakoid ΔpH. Then the absence of oxidized PQ in the intermonomer quinone exchange cavity prevents reduction of PQ at the n-site of the Cyt b_6f complex, by this making CET uncoupled from H^+ translocation.

4. Dark inactivation of FNR activates, rather than inactivates, CET. This suggest that FNR is not involved in the CET pathway.
5. Not CET, but electron transport to alternative electron acceptors, mainly for nitrite and O_2 reduction, is the dominant mechanism for the precise control of ATP/NADPH stoichiometry ratio during photosynthesis.

REFERENCES

1. Albertsson, P.-A. (1995) "The structure and function of the chloroplast photosynthetic membrane – a model for the domain organization." *Photosynth. Res.* **46**: 141–149.
2. Albertsson, P.-A. (2001) "A quantitative model of the domain structure of the photosynthetic membrane." *Trends in Plant Science* **6**: 349–354.
3. Allen, J.F. (2002) "Photosynthesis of ATP electrons, proton pumps, rotors, and poise." *Cell* **110**: 273–276.
4. Allen, J.F. (2003) "Cyclic, pseudocyclic and noncyclic photophosphorylation: new links in the chain." *Trends Plant Sci.* **8**: 15–19.
5. Arnon, D.I. (1955) "The chloroplast as a complete photosynthetic unit." *Science* **122**: 9–16.
6. Arnon, D.I., Allen, M.B., and Whatley, F.R. (1956) "Photosynthesis by isolated chloroplasts. IV. General concept and comparison of three photochemical reactions." *Biochim. Biophys. Acta* **20**: 449–461.
7. Arnon, D.I., Losada, M., Whatley, F.R., Tsujimoto, H.I., Hall, D.O., and Horton, A.A. (1961) "Photosynthetic phosphorylation and molecular oxygen." *Biochemistry* **47**: 1314–1334.
8. Arnon, D.I., Whatley, F.R., and Allen, M.B. (1954) "Photosynthesis by isolated chloroplasts. II. Photosynthetic phosphorylation, the conversion of light into phosphate bond energy." *J. Am. Chem. Soc.* **76**: 6324–29.
9. Arnon, D.I., Whatley, F.R., and Allen, M.B. (1955) "Vitamin K as a cofactor of photosynthetic phosphorylation." *Biochim. Biophys. Acta* **16**: 607–608.
10. Arnon, D.I., Whatley, F.R., and Allen, M.B. (1958) "Assimilatory power in photosynthesis." *Science* **127**: 1026–1034.
11. Arnon, D.I., Whatley, F.R., and Allen, M.B. (1959) "Photosynthesis by isolated chloroplasts. VIII. Photosynthetic photophosphorylation and the generation of assimilatory power." *Biochim. Biophys. Acta* **32**: 47–57.
12. Asada, K. (2006) "Production and scavenging of reactive oxygen species in chloroplasts and their functions." *Plant Physiol.* **141**: 391–396.
13. Backhausen, J.E., Kitzmann, C., and Scheibe, R. (1994) "Competition between electron acceptors in photosynthesis: Regulation of the malate valve during C02 fixation and nitrite reduction." *Photosynth. Res.* **42**: 75–86.
14. Badger, M.R. (1985) "Photosynthetic oxygen exchange." *Ann. Rev. Plant Physiol.* **36**: 27–53.
15. Badger, M.R., von Caemmerer, S., Ruuska, S., and Nakano, H. (2000) "Electron flow to oxygen in higher plants and algae: rate and control of direct photoreduction (Mehler reaction) and Rubisco oxygenase." *Phil. Trans. R. Soc. Lond. B.* **355**: 1433–1446.
16. Baniulis, D., Yamashita, E., Zhang, H., Hasan, S.S., and Cramer, W.A. (2008) "Structure–function of the Cytochrome b6f complex." *Photochem and Photobiol* **84**: 1349–1358.
17. Barber, J. (1998) "Photosystem two." *BBA* **1365**: 269–277.
18. Bassham, J.A., Benson, A.A., and Calvin, M. (1950) "The path of carbon in photosynthesis. VII. The role of malic acid." *J. Biol. Chem.* **185**: 781–7.

19. Baysdorfer, C. and Robinson, J.M. (1985) “Metabolic interactions between spinach leaf nitrite reductase and ferrodoxin-NADP reductase.” *Plant Physiol.* **77**: 318–320.
20. Ben-Shem, A., Frolow, F., and Nelson, N. (2003) “Crystal structure of plant photosystem I.” *Nature* **426**: 630–635.
21. Bendall, D.S. and Manasse, R. (1995) “Cyclic phosphorylation and electron transport.” *Biochim. Biophys. Acta* **1229**: 23–38.
22. Berry, E.A., Kuras, M.G., Huang, L., and Crofts, A.R. (2000) “Structure and function of cytochrome *bc* complexes.” *Annu. Rev. Biochem.* **69**: 1005–1075.
23. Breton, F., Piletska, E.V., Karim, K., Rouillon, R., Piletsky, S.A. (2006) “Mimicking the plastoquinone-b inding pocket of photosystem II using molecularly imprinted polymers.” In *Biotechnological Applications of Photosynthetic Proteins: Biochips, Biosensors and Biodevices* (eds M.T. Giardi & E.V. Piletska), pp. 155–165.
24. Breyton, C., Nandha, B., Johnson, G., Joliot, P., and Finazzi, G. (2006) “Redox modulation of cyclic electron flow around photosystem I in C_3 plants.” *Biochemistry* **45**: 13465–13475.
25. Buchanan, B.B., Gruissem, W., and Jones, R.L. (2000) “Biochemistry & Molecular Biology of Plants.” American Society of Plant Physiologists, Rockville, Maryland.
26. Burns, C.M. and Karplus, A.P. (1994) “Refined crystal structure of spinach ferredoxin reductase at 1.7 Å resolution: oxidized, reduced and 2-Phospho-5-AMP bound states.” *J. Mol. Biol* **247**: 125–45.
27. Buschmann, C., Prehn, H., and Lichtenthaler, H. (1984) “Photoacoustic spectroscopy (PAS) and its application in photosynthesis research.” *Photosynth. Res.* **5**: 29–46.
28. Böhme, H. (1978) “Quantitative determination of ferredoxin, Ferredoxin-NADP reductase and plastocyanin in spinach chloroplasts.” *Eur. J. Biochem.* **83**: 137–141.
29. Campo, F.F., Ramirez, J.M., and Arnon, D.A. (1968) “Stoichiometry of photosynthetic phosphorylation.” *J. Biol. Chem* **243**: 2805–2809.
30. Carrillo, N. and Vallejos, R.H. (1982) “Interaction of ferredoxin-NADP oxidoreductase with the thylakoid membrane.” *Plant Physiol.* **69**: 210213.
31. Cassan, N., Lagouette, B., and Setif, P. (2005) “Ferredoxin-$NADP^+$ reductase. Kinetics of electron transfer, transient intermediates, and catalytic activities studied by flash-absorption spectroscopy with isolated photosystem I and ferredoxin.” *J. Biol. Chem.* **280**: 25960–72.
32. Cha, Y. and Mauzerall, D.C. (1992) “Energy storage of linear and cyclic electron flows in photosynthesis.” *Plant Physiol.* **100**: 1869–1877.
33. Chow, W.S. and Hope, A.B. (1998) “The electrochromic signal, redox reactions in the cytochrome *bf* complex and photosystem functionality in photoinhibited tobacco leaf segments.” *Aust. J. Plant Physiol.* **25**: 775–784.
34. Chow, W.S. and Hope, A.B. (2004a) “Electron fluxes through photosystem I in cucumber leaf discs probed by far-red light.” *Photosynth. Res.* **81**: 77–89.
35. Chow, W.S. and Hope, A.B. (2004b) “Kinetics of reactions around the cytochrome bf complex studied in intact leaf disks.” *Photosynth. Res.* **81**: 153–163.
36. Clark, R.D., Hawkesford, M.J., Coughlan, S.J., Bennett, J., and Hind, G. (1984) “Association of ferredoxin-NADP+ oxidoreductase with the chloroplast cytochrome b-f complex.” *FEBS* **174**: 137–42.

13

37. Cruz, J.A., Avenson, T.J., Kanazawa, A., Takizawa, K., Edwards, G.E., and Kramer, D.M. (2005) "Plasticity in light reactions of photosynthesis for energy production and photoprotection." *J. Exp. Bot.* **56**: 395–406.
38. Cruz, J.A., Sacksteder, C.A., Kanazawa, A., and Kramer, D.M. (2001) "Contribution of electric field ($\Delta\psi$) to steady-state transthylakoid proton motive force (*pmf*) in vitro and in vivo. Control of *pmf* parsing into $\Delta\psi$ and ΔpH by ionic strength." *Biochemistry* **40**: 1226–1237.
39. Fan, D.-Y., Nie, Q., Hope, A.B., Hillier, W., Pogson, B.J., and Chow, W.S. (2007) "Quantification of cyclic electron flow around Photosystem I in spinach leaves during photosynthetic induction." *Photosynth Res* **94**: 347–357.
40. Finazzi, G., Sommer, F., and Hippler, M. (2005) "Release of oxidized plastocyanin from photosystem I limits electron transfer between photosystem I and cytochrome b6f complex in vivo." *Proc. Natl. Acad. Sci. USA* **102**: 7031–7036.
41. Fork, D.C. and Herbert, S.K. (1991) "A gas-permeable photoacoustic cell." *Photosynth. Res.* **27**: 151–6.
42. Fukuyama, K. (2004) "Structure and function of plant-type ferredoxins." *Photosynth Res* **81**: 289–301.
43. Genty, B., Briantais, J.M., and Baker, N.R. (1989) "The relationship between quantum yield of photosynthetic electron transport and quenching of chlorophyll fluorescence." *Biochem. Biophys. Acta* **990**: 87–92.
44. Golding, A.J., Joliot, P., and Johnson, G.N. (2005) "Equilibration between cytochrome f and P700 in intact leaves." *Biochim. Biophys. Acta* **1706**: 105–109.
45. Gupta, R., He, Z., and Luan, S. (2002) "Functional relationship of cytochrome c6 and plastocyanin in Arabidopsis." **417**: 567–571.
46. Guskov, A., Kern, J., Gabdulkhakov, A., Broser, M., Zouni, A., and Saenger, W. (2009) "Cyanobacterial photosystem II at 2.9–A resolution and the role of quinones, lipids, channels and chloride." *Nature Str. Mol. B.* **16**: 334–342.
47. Haldrup, A., Navel, H., and Scheller, H.V. (1999) "The interaction between plastocyanin and photosystem I is inefficient in transgenic Arabidopsis plants lacking the PSI-N subunit of photosystem I." *Plant J.* **17**: 689–698.
48. Hanke, G.T., Kurisu, G., Kusunoki, M., and Hase, T. (2004) "Fd : FNR electron transfer complexes: evolutionary refinement of structural interactions." *Photosynth Res* **81**: 317–327.
49. Harbinson, J. and Hedley, C.L. (1989) "The kinetics of P 700+ reduction in leaves: a novel in situ probe of thylakoid functioning." *Plant, Cell Env.* **12**: 357–369.
50. Hase, T., Schürmann, P., Knaff, D.B. (2006) "The interaction of ferredoxin with ferredoxin-dependent enzymes." In *Photosystem I* (ed J.H. Golbeck), pp. 477–98. Springer.
51. Hauska, G., Schütz, Büttner, L. (1996) "The cytochrome b_6f complex – composition, structure and function." In *Oxygenic Photosynthesis: The Light Reactions* (eds D.R. Ort & C.F. Yocum), pp. 477–398. Kluwer Acad. Publishers, Dordrecht/ Boston/London.
52. Havaux, M. (1992) "Photoacoustic measurements of cyclic electron flow around photosystem I in leaves adapted to light-states 1 and 2." *Plant Cell Physiol.* **33(6)**: 799–803.
53. Heber, U. (2002) "Irrungen, Wirrungen? The Mehler reaction in relation to cyclic electron transport in C3 plants." *Photosynth Res* **73**: 223–231.

54. Heber, U., Gerst, U., Krieger, A., Neimanis, S., and Kobayashi, Y. (1995) "Coupled cyclic electron transport in intact chloroplasts and leaves of C_3 plants: Does it exist? if so, what is its function?" *Photosynthesis Research* **46**: 269–275.
55. Herbert, S., Fork, D.C., and Malkin, S. (1990) "Photoacoustic measurements in vivo of energy storage by cyclic electron flow in algae and higher plants." *Plant Physiology* **94**: 926–934.
56. Hill, R. and Bendall, F. (1960) 0147Function of the two cytochrome components in chloroplasts: a working hypothesis." *Nature* **186**: 40–44.
57. Hillier, W. and Babcock, G.T. (2001) "Photosynthetic reaction centers." *Plant Physiol* **125**: 33–37.
58. Hisabori, T., Ueoka-Nakanishib, H., Konnob, H., and Koyamab, F. (2003) "Molecular evolution of the modulator of chloroplast ATP synthase: origin of the conformational change dependent regulation." *FEBS letters* **545**: 71–75.
59. Hope, A.B. and Morland, A. (1980) "Electrogenic events in chloroplasts and their relation to the electrochromic shift (P518)." *Aust. J. Plant Physiol.* **7**: 699–711.
60. Hosler, J.P. and Yocum, C.F. (1985) "Evidence for two cyclic photo-phosphorylation reactions concurrent with ferrodoxin-catalyzed non-cyclic electron transport." *Biochim. Biophys. Acta* **808**: 21–31.
61. Hosler, J.P. and Yocum, C.F. (1987) "Regulation of cyclic photophosphorylation during ferredoxin-mediated electron transport." *Plant Physiol.* **83**: 965–969.
62. Joet, T., Cournac, L., Horvath, E.M., Medgyesy, P., and Peltier, G. (2001) "Increased sensitivity of photosynthesis to Antimycin A induced by inactivation of the chloroplast *ndhB* gene. Evidence for a participation of the NADH-dehydrogenase complex to cyclic electron flow around photosystem I." *Plant Phys* **125**: 1919–29.
63. Joët, T., Cournac, L., Peltier, G., and Havaux, M. (2002) "Cyclic electron flow around photosystem I in C_3 plants. In vivo control by the redox state of chloroplasts and involvement of the NADH-dehydrogenase complex." *Plant Physiology* **128**: 760–769.
64. Johnson, G.N. (2005) "Cyclic electron transport in C_3 plants: fact or artefact?" *J. Exp. Bot.* **56**: 407–416.
65. Joliot, P., Béal, D., and Joliot, A. (2004) "Cyclic electron flow under saturating excitation of dark-adapted Arabidopsis leaves." *Biochim. Biophys. Acta* **1656**: 166–176.
66. Joliot, P. and Joliot, A. (1984) "Electron transfer between the two photosystems I. Flash excitation under oxidizing conditions." *BBA* **765**: 210–218.
67. Joliot, P. and Joliot, A. (2001) "Electrogenic events associated with electron and proton transfers within the cytochrome *b6/f* complex." *Biochim. Biophys. Acta* **1503**: 369–376.
68. Joliot, P. and Joliot, A. (2002) "Cyclic electron transfer in plant leaf." *PNAS* **99**: 10209–10214.
69. Joliot, P. and Joliot, A. (2006) "Cyclic electron flow in C3 plants." *Biochim. Biophys. Acta* **1757**: 362–368.
70. Joy, K.W. and Hageman, R.H. (1966) "The purification and properties of nitrite reductase from higher plants, and its dependence on ferredoxin." *Biochem. J.* **100**: 263–73.
71. Kanazawa, A. and Kramer, D.M. (2002) "*In vivo* modulation of nonphotochemical exciton quenching (NPQ) by regulation of the chloroplast ATP synthase." *PNAS* **99**: 12789–12794.

72. Karplus, P.A. and Faber, H.R. (2004) “Structural aspects of plant ferredoxin : NADP+ oxidoreductases.” *Phothosynt Res* **81**: 303–315.
73. Kirchhoff, H., Schöttler, M.A., and Maurer, J.W.E. (2004) “Plastocyanin redox kinetics in spinach chloroplasts: evidence for disequilibrium in the high potential chain.” *Biochim. Biophys. Acta* **1659**: 63–72.
74. Klughammer, C. and Schreiber, U. (1991) “Analysis of light-induced absorbance changes in the near-infrared spectral region. I. Characterization of various components in isolated chloroplasts.” *Z. Naturforsch* **46c**: 233–244.
75. Kobayashi, Y. and Heber, U. (1994) “Rates of vectorial proton transport supported by cyclic electron flow during oxygen reduction by illuminated intact chloroplasts.” *Photosynth. Res.* **41**: 419–428.
76. Kok, B., Forbush, M., and McGloin, M. (1970) “Cooperation of charges in photosynthetic oxygen evolution.” *Photochem. Photobiol.* **11**: 457–475.
77. Kramer, D.M. and Sacksteder, C.A. (1998) “A diffused-optics flash kinetics spectrophotometer (DOFS) for measurements of absorbance changes in intact plants in the steady state.” *Photosynth. Res.* **56**: 103–112.
78. Laisk, A., Eichelmann, H., Oja, V., Rasulov, B., and Rämma, H. (2006) “Photosystem II cycle and alternative electron flow in leaves.” *Plant Cell Physiol* **47**: 972–83.
79. Laisk, A., Oja, V., Rasulov, B., Rämma, H., Eichelmann, H., Kasparova, I., Pettai, H., Padu, E., and Vapaavuori, E. (2002) “A computer-operated routine of gas exchange and optical measurements to diagnose photosynthetic apparatus in leaves.” *Plant Cell Env.* **25**: 923–943.
80. Lintala, M., Allahverdiyeva, Y., Kidron, H., Piippo, M., Battchikova, N., Suorsa, M., Rintamäki, E., Salminen, T.A., Aro, E.-M., and Mulo, P. (2007) “Structural and functional characterization of ferredoxin-NADP+-oxidoreductase using knock-out mutants of Arabidopsis.” *Plant J.* **49**: 1041–1052.
81. McCarty, R.E. (2005) “ATP synthase of chloroplast thylakoid membranes: a more in depth characterization of its ATPase activity.” *J. Bioen. Biomemb.* **37**: 289–97.
82. McCauley, S.W. and Melis, A. (1986) “Quantitation of plastoquinone photoreduction in spinach chloroplasts.” *Photosynth. Res.* **8**: 3–16.
83. Melis, A. and Brown, J.S. (1980) “Stoichiometry of system I and system II reaction centers and of plastoquinone in different photosynthetic membranes.” *PNAS* **77**: 4712–6.
84. Mitchell, P. (1966) “Chemiosmotic coupling in oxidative and photosynthetic phosphorylation.” *Biol. Rev.* **41**: 445–502.
85. Mitchell, P. (1975a) “The protonmotive Q cycle: A general formulation.” *FEBS letters* **59**: 137–9.
86. Mitchell, P. (1975b) “Protonmotive redox mechanism of the cytochrome b-c_l complex in the respiratory chain: protonmotive ubiquinone cycle.” *FEBS letters* **56**: 1–6.
87. Munekage, Y., Hashimoto, M., Miyake, C., Tomizawa, K.-I., Endo, T., Tasaka, M., and Shikanai, T. (2004) “Cyclic electron flow around photosystem I is essential for photosynthesis.” *Nature* **429**: 579–582.
88. Musiani, F., Dikiy, A., Semenov, A.Y., and Ciurli, S. (2005) “Structure of the intermolecular complex between plastocyanin and pytochrome *f* from spinach.” *J. Biol. Chem.* **280**: 18833–18841.
89. Nelson, N. and Yocum, C.F. (2006) “Structure and function of photosystems I and II.” *Annu. Rev. Plant Biol* **57**: 521–565.

90. Neuhaus, H.E. and Emes, M.J. (2000) “Nonphotosynthetic metabolism in plastids.” *Annu. Rev. Plant Physiol.* **51**: 111–40.
91. Noctor, G. and Foyer, C.H. (1998) “A re-evaluation of the ATP:NADPH budget during C_3 photosynthesis: a contribution from nitrate assimilation and its associated respiratory activity?” *J. Exp. Bot.* **49**: 1895–1908.
92. Oja, V., Bichele, I., Hüve, K., Rasulov, B., and Laisk, A. (2004) “Reductive titration of photosystem I and differential extinction coefficient of $P700^+$ at 810–950 nm in leaves.” *Biochim. Biophys. Acta* **1658**: 225–234.
93. Oja, V., Eichelmann, H., Peterson, R.B., Rasulov, B., and Laisk, A. (2003) “Decyphering the 820 nm signal: redox state of donor side and quantum yield of photosystem I in leaves.” *Photosynth. Res.* **78**: 1–15.
94. Patel, P.K., Bendall, D.S., and Ridley, S.M. (1986) “Site of action of a halogenated 4-hydroxypyridine on ferredoxin-catalysed cyclic photophosphorylation.” *FEBS* **206**: 249–252.
95. Rich, P.R. (1988) “A critical examination of the supposed variable proton stoichiometry of the chloroplast cytochrome b/f complex.” *Biochim. Biophys. Acta* **932**: 33–42.
96. Rich, P.R., Madgwick, S.A., and Moss, D.A. (1991) “The interactions of duroquinol, DBMIB and NQNO with the chloroplast cytochrome bf complex.” *Biochim Biophys Acta* **1058**: 312–328.
97. Richter, M.L., Samra, H.S., He, F., Giessel, A.J., and Kuczera1, K.K. (2005) “Coupling proton movement to ATP synthesis in the chloroplast ATP synthase.” *J. Bioenerg. Biomemb.* **37**: 467–73.
98. Robinson, J.M. (1986) “Carbon dioxide and nitrite photoassimilatory processes do not intercompete for reducing equivalents in spinach and soybean leaf chloroplasts.” *Plant Physiol.* **80**: 676–684.
99. Robinson, J.M. (1990) “Nitrite photoreduction in vivo is inhibited by oxygen.” *Plant Physiol* **92**: 862–865.
100. Ruhle, W., Pschorn, R., and Wild, A. (1988) “Regulation of the photosynthetic electron transport during dark-light transitions by activation of the ferrodoxin-NADP+-oxidoreductase in higher plants.” *Photosynth. Res.* **11**: 161–171.
101. Rumberg, B., Schubert, K., Strelow, F., and Tran-Anh, T. (1990) “The H^+/ATP coupling ratio at the H^+-ATP-synthase of spinach chloroplasts is four.” 125–128.
102. Sacksteder, C.A., Kanazawa, A., Jacoby, M.E., and Kramer, D.M. (2000) “The proton to electron stoichiometry of steady-state photosynthesis in living plants: a proton-pumping Q cycle is continuously engaged.” *PNAS* **97**: 14283–14288.
103. Sawaya, M.R. and Merchant, S. (2005) “The light reactions: a guide to recent acquisitions for the picture gallery.” *The Plant Cell* **17**: 648–63.
104. Sazanov, L.A., Burrows, P.A., and Nixon, P.J. (1998) “The chloroplast Ndh complex mediates the dark reduction of the plastoquinone pool in response to heat stress in tobacco leaves.” *FEBS letters* **429**: 115–118.
105. Schansker, G., Srivastava, A., Govindjee, and Strasser, R.J. (2003) “Characterization of the 820-nm transmission signal paralleling the chlorophyll a fluorescence rise (OJIP) in pea leaves.” *Functional Plant Biology* **30**: 785–796.
106. Scheibe, R. (1987) “$NADP^+$-malate dehydrogenase in C_3-plants: Regulation and role of a light-activated enzyme.” *Physiologia Plantarum* **71**: 393–400.
107. Scheller, H.V. (1996) “In vitro cyclic electron transport in barley thylakoids follows two independent pathways.” *Plant Physiol.* **110**: 187–194.

14

108. Scheuring, S., Fotiadis, D., Möller, C., Müller, S.A., Engel, A., and Müller, D.J. (2001) "Single proteins observed by atomic force microscopy." *Single Mol.* **2**: 59–67.
109. Seelert, H., Dencher, N.A., and Müller, D.J. (2003) "Fourteen protomers compose the oligomer II of the proton-rotor in spinach chloroplast ATP synthase." *J. Mol. Biol.* **333**: 337–344.
110. Seelert, H., Poetsch, A., Dencher, N.A., Engel, A., Stahlberg, H., and Müller, D.J. (2000) "Proton powered turbine of a plant motor." *Nature* **405**: 418–419.
111. Shin, M. (2004) "How is ferredoxin-NADP reductase involved in the NADP photoreduction of chloroplasts?" *Photosynth. Res.* **80**: 307–313.
112. Siebke, K., Ghannoum, O., Conroy, J.P., Badger, M.R., and von Caemmerer, S. (2003) "Photosynthetic oxygen exchange in C_4 grasses: the role of oxygen as electron acceptor." *Plant Cell Env.* **26**: 1963–1972.
113. Siggel, U. (1974) "The control of electron transport by two pH-sensitive sites." In *Proc. 3-rd Internat. Congr. on Photosynth.* (ed M. Avron), pp. 645–654. Elsevier, Amsterdam.
114. Silva de D.G.A.H., Beoku-Betts D., Kyritsis P., Govindaraju K., Powls R., Tomkinson N.P., and Sykes A.G. (1992) "Protein-protein cross-reactions involving plastocyanin, cytochrome f and azurin: self-exchange rate constants and related studies with inorganic complexes." *J. Chem. Soc. Dalton Trans* 2145–2151.
115. Steigmiller, S., Turina, P., and Gräber, P. (2008) "The thermodynamic H^+/ATP ratios of the H^+-ATPsynthases from chloroplasts and *Escherichia coli*." *PNAS* **105**: 3745–50.
116. Tagawa, K., Tsujimoto, H.Y., and Arnon, D.I. (1963) "Role of chloroplast ferredoxin in the energy conversion process of photosynthesis." *Proc. Natl. Acad. Sci. USA* **49**: 567–572.
117. Talts, E., Oja, V., Rämma, H., Rasulov, B., Anijalg, A., and Laisk, A. (2007) "Dark inactivation of ferredoxin-NADP reductase and cyclic electron flow under far-red light in sunflower leaves." *Photosynth. Res.* **94**: 109–120.
118. Whitmarsh, J. and Ort, D.R. (1984) "Stoichiometries of electron transport complexes in spinach chloroplasts." *Archives of Biochemistry and Biophysics* **231**: 378–389.
119. Yamamoto, H., Kato, H., Shinazaki, Y., Horiguchi, S., Shikanai, T., Hase, T., Endo, T., Nishioka, M., Makino, A., Tomizawa, K., and Miyake, C. (2006) "Ferredoxin limits cyclic electron flow around PSI (CEF-PSI) in higher plants – stimulation of CEF-PSI enhances non-photochemical quenching of Chl fluorescence in transplastomic tobacco." *Plant Cell Physiol.* **47**: 1355–71.
120. Yoshida, M., Muneyuki, E., and Hisabori, T. (2001) "ATP synthase – a marvellous rotary engine of the cell." *Nature reviews Mol. Cell. Biol.* **2**: 669–77.
121. Zhang, H., Whitelegge, J.P., and Cramer, W.A. (2001) "Ferredoxin:NADP+ oxidoreductase is a subunit of the chloroplast cytochrome b6f complex." *J. Biol. Chem.* **276**: 38159–38165.

SUMMARY IN ESTONIAN

Tsükliline elektrontransport taimedes – selle mõõtmine ning mehhanism

Fotosüntees on oluline ainevahetusprotsess, mis võimaldab toota orgaanilisi aineid valgusenergia kaasabil. Fotosünteesi esimeseks reaktsiooniks on vee oksüdeerimine, mille tulemusel vabanevad prootonid, elektronid ja molekulaarne hapnik. Selleks, et redutseerida 1 CO_2 molekul suhkru tasemele kasutatakse ära 2 H_2O molekulist saadud 4 elektroni. Suhkru sünteesiks ei piisa ainult CO_2 redutseerimisest, vaja läheb ka 3 ATP molekuli energiat. Paraku peab kõik CO_2 redutseerimiseks vajaminev ATP olema toodetud fotosünteesi enda poolt. Kui fotosünteesis kasutataks ka mitokondriaalseid ressursse, siis tarvitaks fotosüntees ära suure osa iseenda poolt toodetavast produktist, vähendades oluliselt suhkrute sünteesi. Seetõttu on ATP sünteesi ja elektrontranspordi vaheline stöhhiomeetria fotosünteesis väga oluline.

ATPd sünteesitakse tülakoidide membraanis asuva ATPaasi poolt, mis kasutab selleks valgusreaktsioonide käigus tekkinud prootongradiendi energiat. Prootongradient formeerub vee lagundamise (1 H^+) ja spetsiifiliselt organiseeritud elektrontranspordi (2 H^+) toimel. Seega kantakse 1 elektroni kohta 3 H^+ läbi membraani, mis teeb 4 elektroni (ehk 2 NADPH) kohta 12 H^+. Kuigi viimased andmed näitavad, et ATPaasi prootonitarve on ikkagi 4 H^+ : 1 ATP, mitte rohkem, on selle üle vaieldud vähemalt pool sajandit. Samuti eksisteerivad kloroplastides teisedki ATP energiat nõudvad protsessid peale CO_2 redutseerimise, nagu näiteks tärklise ning valgusüntees. Seetõttu on ATP lisatootmine fotosünteesi protsessis jätkuvalt kõneaineks.

Alates 1950-ndatest aastatest on juurdunud üldine usk, et elektrontranspordi ajal võib osa elektrone suunata tagasi nii, et need on suutelised veel kord prootoneid üle kandma. Seda protsessi on hakatud nimetama tsükliliseks elektrontranspordiks (CET) ning arvatakse, et CET võimaldab sünteesida ATPd juurde "nii palju kui tarvis". Käesolev töö keskendubki tsüklilise elektrontranspordi mõõtmisele suhteliselt uute ja täpsete meetoditega, CETi mõju hindamisele ja selle võimalikule seosele prootongradiendi formeerumisel.

Kasutades TÜ MRI biofüüsika ja taimefüsioloogia õppetooli unikaalset aparatuuri ning metoodikaid toimusid käesoleva töö esimesed CET mõõtmised eelnevalt pimeduses hoitud päevalille lehtedes kaugpunase valguse all (FRL – 720 nm). Kuna FRL ergastab peamiselt fotosüsteemi I (PSI), siis oli see soodne olukord CET mõõtmiseks, mis toimubki ümber PSI. Tulemused näitasid, et CET oli aeglasem peale lühikesi pimeperioode, kuid kiirenens peale pikemaid (>200s). Järeldasime, et pimeduses inaktiveerub ferredoksiin-NADP reduktaas (FNR) – ensüüm mis katalüüsib elektronide edasiliikumist PSI-lt – põhjustades elektronide kiirenenud tagasivoolu. Järgmistes katsetes pidurdasime elektronide edasivoolu aktseptori puudumisega, rakendades väga madalalid CO_2 ja O_2

kontsentratsioone. Tulemused näitasid, et CET kiirenes ka elektronide aktseptori puudumisel.

Nendes katsetes rakendatud väga madalate CO_2 ja O_2 kontsentratsioonide juures oli ATP vajadus fotosünteesis nullilähedane, ometi registreerisime väga kiiret CET. Selles olukorras oli võimatu seletada, kus tarbitakse CET abil sünteesitud ATP? Järeldasime, et nendes katsetingimustes registreeritud kiire CET ei olnudki seotud prootonite transpordi ja ATP sünteesiga, vaid täitis pigem kaitsefunktsiooni, võimaldades elektronidel ringeldes valgusenergiat soojuseks dissipeerida ka aktseptori puudumisel. Seda ideed toetasid võrdlus-katsed kaugpunase (FRL ergastab suures osas ainult PSI) ja rohelise (ergastab PSI ja PSII võrdselt) valgusega, mis näitasid ligikaudu võrdset prootongradiendi taset hoolimata sellest, et FRL indutseeris kiire CET, roheline valgus aga üldse mitte. Nende ja veel mitmete teiste katsete alusel on käesoleva töö raames edasi arendatud CETi raja mudelit, mis on esitatud nüüd järgmiselt: ferredoksiin (või PSI-ga seondunud FeS e^- kandjad) → FNR (osalus on küsitav) → Cyt c_n → Cyt c_h → Cyt c_l → Rieske FeS → Cyt f → Plastotsüaniin → P700 → (FeS kompleks) → Ferredoksiin. See on sisuliselt Q-tsükli pööre, mis eeldab, et elektronid võivad liikuda PSI aktseptorpoolelt doonorpoolele tagasi läbi tsütokroom b_6f kompleksi transportides prootoneid olukorras, kus prootongradient on madal, mitte transportides neid aga olukorras, kus prootongradient on niigi kõrge.

ACKNOWLEDGEMENTS

First of all I would like to thank my supervisor prof. Agu Laisk for the interesting time of PhD studies spent under his supervision. I am grateful that he gave me the opportunity to do my research in his lab and provided me his support.

I would also like to thank my colleagues who where always available for help and discussion: Arvi Freiberg, Vello Oja, Evi Padu, Hillar Eichelmann, Irina Bichele, Bakhtier Rasulov, Heikko Rämma.

Finally greatest thanks to my family and friends who helped me emotionally.

15

PUBLICATIONS

CURRICULUM VITAE

Eero Talts

Date and place of birth	28.01.1981, Pärnu
Address	Pirni 2, MRI, LOTE, University of Tartu
Email	outsider@ut.ee

Education and professional employment

1991–1999	Pärnu Koidula Gymnasium.
1999–2003	University of Tartu, Gene Technology BSc.
2003–2005	University of Tartu, Molecular and Cellular Biology, MSc.
2005–2010	University of Tartu, Molecular and Cellular Biology, PhD.
2006– ...	technician; Department of biophysics and plant physiology, LOTE.

Scientific work

I started my research in molecular biology-oriented biochemistry laboratory, where I studied yeast mitochondrial DNA. The subsequent interest has been the photosynthesis of plants, using physical and biochemical measurements. I have dealt with a lot of IT problems and computer programming.

List of publications

1. **Talts, E.**, Oja, V., Rämma, H., Rasulov, B., Anijalg, A. and Laisk A. (2007) "Dark inactivation of ferredoxin-NADP reductase and cyclic electron flow under far-red light in sunflower leaves." Photosynth Res 94:109–120.
2. Laisk, A., Eichelmann, H., Oja, V., **Talts E.**, and Scheibe, R. (2007) "Rates and roles of cyclic and alternative electron flow in potato leaves." Plant Cell Physiol 48(11): 1575–588.
3. Eichelmann, H., **Talts, E.**, Oja, V., Padu, E. and Laisk, A. (2009) "Rubisco *in planta* k_{cat} is regulated in balance with photosynthetic electron transport." J. Exp. Botany 60:4077–4088.
4. Laisk, A., **Talts, E.**, Oja, V., Eichelmann, H., and Peterson, R.B. (2010) "Fast cyclic electron transport around photosystem I in leaves under far-red light: a proton-uncoupled pathway?" Photosynth Res 103:79–95.

CURRICULUM VITAE

Eero Talts

Sünniaeg ja koht	28.01.1981, Pärnu
Aadress	Pirni 2, MRI, LOTE, Tartu Ülikool
Email	outsider@ut.ee

Haridus ja erialane teenistuskäik

1991–1999	Pärnu Koidula Gümnaasium.
1999–2003	Tartu Ülikool, Geenitehnoloogia BSc.
2003–2005	Tartu Ülikool, Molekulaar- ja rakubioloogia MSc.
2005–2010	Tartu Ülikool, Molekulaar- ja rakubioloogia PhD.
2006– ...	laborant; Biofüüsika- ja taimefüsioloogia õppetool, TÜMRI

Teadustegevus

Alustasin oma teadustegevusega molekulaarbioloogia suunitlusega biokeemia laboris, kus uurisin pärmi mitogondriaalset DNA-d. Hilisemaks uurimistemaatikaks on olnud taimede fotosüntees kasutades füüsikalisi ja biokeemilisi mõõtmisi. Olen tegelenud palju ka infotehnoloogiliste probleemide ning programmeerimisega.

Publikatsioonid

1. **Talts, E.**, Oja, V., Rämma, H., Rasulov, B., Anijalg, A. and Laisk A. (2007) "Dark inactivation of ferredoxin-NADP reductase and cyclic electron flow under far-red light in sunflower leaves." Photosynth Res 94:109–120.
2. Laisk, A., Eichelmann, H., Oja, V., **Talts E.**, and Scheibe, R. (2007) "Rates and roles of cyclic and alternative electron flow in potato leaves." Plant Cell Physiol 48(11): 1575–588.
3. Eichelmann, H., **Talts, E.**, Oja, V., Padu, E. and Laisk, A. (2009) "Rubisco *in planta* k_{cat} is regulated in balance with photosynthetic electron transport." J. Exp. Botany 60:4077–4088.
4. Laisk, A., **Talts, E.**, Oja, V., Eichelmann, H., and Peterson, R.B. (2010) "Fast cyclic electron transport around photosystem I in leaves under far-red light: a proton-uncoupled pathway?" Photosynth Res 103:79–95.

DISSERTATIONES BIOLOGICAE UNIVERSITATIS TARTUENSIS

1. **Toivo Maimets**. Studies of human oncoprotein p53. Tartu, 1991, 96 p.
2. **Enn K. Seppet**. Thyroid state control over energy metabolism, ion transport and contractile functions in rat heart. Tartu, 1991, 135 p.
3. **Kristjan Zobel**. Epifüütsete makrosamblike väärtus õhu saastuse indikaatoritena Hamar-Dobani boreaalsetes mägimetsades. Tartu, 1992, 131 lk.
4. **Andres Mäe**. Conjugal mobilization of catabolic plasmids by transposable elements in helper plasmids. Tartu, 1992, 91 p.
5. **Maia Kivisaar**. Studies on phenol degradation genes of *Pseudomonas* sp. strain EST 1001. Tartu, 1992, 61 p.
6. **Allan Nurk**. Nucleotide sequences of phenol degradative genes from *Pseudomonas sp.* strain EST 1001 and their transcriptional activation in *Pseudomonas putida.* Tartu, 1992, 72 p.
7. **Ülo Tamm**. The genus *Populus* L. in Estonia: variation of the species biology and introduction. Tartu, 1993, 91 p.
8. **Jaanus Remme**. Studies on the peptidyltransferase centre of the *E.coli* ribosome. Tartu, 1993, 68 p.
9. **Ülo Langel**. Galanin and galanin antagonists. Tartu, 1993, 97 p.
10. **Arvo Käärd**. The development of an automatic online dynamic fluorescense-based pH-dependent fiber optic penicillin flowthrought biosensor for the control of the benzylpenicillin hydrolysis. Tartu, 1993, 117 p.
11. **Lilian Järvekülg**. Antigenic analysis and development of sensitive immunoassay for potato viruses. Tartu, 1993, 147 p.
12. **Jaak Palumets**. Analysis of phytomass partition in Norway spruce. Tartu, 1993, 47 p.
13. **Arne Sellin**. Variation in hydraulic architecture of *Picea abies* (L.) Karst. trees grown under different enviromental conditions. Tartu, 1994, 119 p.
13. **Mati Reeben**. Regulation of light neurofilament gene expression. Tartu, 1994, 108 p.
14. **Urmas Tartes**. Respiration rhytms in insects. Tartu, 1995, 109 p.
15. **Ülo Puurand**. The complete nucleotide sequence and infections *in vitro* transcripts from cloned cDNA of a potato A potyvirus. Tartu, 1995, 96 p.
16. **Peeter Hõrak**. Pathways of selection in avian reproduction: a functional framework and its application in the population study of the great tit (*Parus major*). Tartu, 1995, 118 p.
17. **Erkki Truve**. Studies on specific and broad spectrum virus resistance in transgenic plants. Tartu, 1996, 158 p.
18. **Illar Pata**. Cloning and characterization of human and mouse ribosomal protein S6-encoding genes. Tartu, 1996, 60 p.
19. **Ülo Niinemets**. Importance of structural features of leaves and canopy in determining species shade-tolerance in temperature deciduous woody taxa. Tartu, 1996, 150 p.

20. **Ants Kurg**. Bovine leukemia virus: molecular studies on the packaging region and DNA diagnostics in cattle. Tartu, 1996, 104 p.
21. **Ene Ustav**. E2 as the modulator of the BPV1 DNA replication. Tartu, 1996, 100 p.
22. **Aksel Soosaar**. Role of helix-loop-helix and nuclear hormone receptor transcription factors in neurogenesis. Tartu, 1996, 109 p.
23. **Maido Remm**. Human papillomavirus type 18: replication, transformation and gene expression. Tartu, 1997, 117 p.
24. **Tiiu Kull**. Population dynamics in *Cypripedium calceolus* L. Tartu, 1997, 124 p.
25. **Kalle Olli**. Evolutionary life-strategies of autotrophic planktonic microorganisms in the Baltic Sea. Tartu, 1997, 180 p.
26. **Meelis Pärtel**. Species diversity and community dynamics in calcareous grassland communities in Western Estonia. Tartu, 1997, 124 p.
27. **Malle Leht**. The Genus *Potentilla* L. in Estonia, Latvia and Lithuania: distribution, morphology and taxonomy. Tartu, 1997, 186 p.
28. **Tanel Tenson**. Ribosomes, peptides and antibiotic resistance. Tartu, 1997, 80 p.
29. **Arvo Tuvikene**. Assessment of inland water pollution using biomarker responses in fish *in vivo* and *in vitro*. Tartu, 1997, 160 p.
30. **Urmas Saarma**. Tuning ribosomal elongation cycle by mutagenesis of 23S rRNA. Tartu, 1997, 134 p.
31. **Henn Ojaveer**. Composition and dynamics of fish stocks in the gulf of Riga ecosystem. Tartu, 1997, 138 p.
32. **Lembi Lõugas**. Post-glacial development of vertebrate fauna in Estonian water bodies. Tartu, 1997, 138 p.
33. **Margus Pooga**. Cell penetrating peptide, transportan, and its predecessors, galanin-based chimeric peptides. Tartu, 1998, 110 p.
34. **Andres Saag**. Evolutionary relationships in some cetrarioid genera (Lichenized Ascomycota). Tartu, 1998, 196 p.
35. **Aivar Liiv**. Ribosomal large subunit assembly *in vivo*. Tartu, 1998, 158 p.
36. **Tatjana Oja**. Isoenzyme diversity and phylogenetic affinities among the eurasian annual bromes (*Bromus* L., Poaceae). Tartu, 1998, 92 p.
37. **Mari Moora**. The influence of arbuscular mycorrhizal (AM) symbiosis on the competition and coexistence of calcareous crassland plant species. Tartu, 1998, 78 p.
38. **Olavi Kurina**. Fungus gnats in Estonia (*Diptera: Bolitophilidae, Keroplatidae, Macroceridae, Ditomyiidae, Diadocidiidae, Mycetophilidae*). Tartu, 1998, 200 p.
39. **Andrus Tasa**. Biological leaching of shales: black shale and oil shale. Tartu, 1998, 98 p.
40. **Arnold Kristjuhan.** Studies on transcriptional activator properties of tumor suppressor protein p53. Tartu, 1998, 86 p.

41. **Sulev Ingerpuu.** Characterization of some human myeloid cell surface and nuclear differentiation antigens. Tartu, 1998, 163 p.
42. **Veljo Kisand.** Responses of planktonic bacteria to the abiotic and biotic factors in the shallow lake Võrtsjärv. Tartu, 1998, 118 p.
43. **Kadri Põldmaa.** Studies in the systematics of hypomyces and allied genera (Hypocreales, Ascomycota). Tartu, 1998, 178 p.
44. **Markus Vetemaa.** Reproduction parameters of fish as indicators in environmental monitoring. Tartu, 1998, 117 p.
45. **Heli Talvik.** Prepatent periods and species composition of different *Oesophagostomum* spp. populations in Estonia and Denmark. Tartu, 1998, 104 p.
46. **Katrin Heinsoo.** Cuticular and stomatal antechamber conductance to water vapour diffusion in *Picea abies* (L.) karst. Tartu, 1999, 133 p.
47. **Tarmo Annilo.** Studies on mammalian ribosomal protein S7. Tartu, 1998, 77 p.
48. **Indrek Ots.** Health state indicies of reproducing great tits (*Parus major*): sources of variation and connections with life-history traits. Tartu, 1999, 117 p.
49. **Juan Jose Cantero.** Plant community diversity and habitat relationships in central Argentina grasslands. Tartu, 1999, 161 p.
50. **Rein Kalamees.** Seed bank, seed rain and community regeneration in Estonian calcareous grasslands. Tartu, 1999, 107 p.
51. **Sulev Kõks.** Cholecystokinin (CCK) — induced anxiety in rats: influence of environmental stimuli and involvement of endopioid mechanisms and erotonin. Tartu, 1999, 123 p.
52. **Ebe Sild.** Impact of increasing concentrations of O_3 and CO_2 on wheat, clover and pasture. Tartu, 1999, 123 p.
53. **Ljudmilla Timofejeva.** Electron microscopical analysis of the synaptonemal complex formation in cereals. Tartu, 1999, 99 p.
54. **Andres Valkna.** Interactions of galanin receptor with ligands and G-proteins: studies with synthetic peptides. Tartu, 1999, 103 p.
55. **Taavi Virro.** Life cycles of planktonic rotifers in lake Peipsi. Tartu, 1999, 101 p.
56. **Ana Rebane.** Mammalian ribosomal protein S3a genes and intron-encoded small nucleolar RNAs U73 and U82. Tartu, 1999, 85 p.
57. **Tiina Tamm.** Cocksfoot mottle virus: the genome organisation and translational strategies. Tartu, 2000, 101 p.
58. **Reet Kurg.** Structure-function relationship of the bovine papilloma virus E2 protein. Tartu, 2000, 89 p.
59. **Toomas Kivisild.** The origins of Southern and Western Eurasian populations: an mtDNA study. Tartu, 2000, 121 p.
60. **Niilo Kaldalu.** Studies of the TOL plasmid transcription factor XylS. Tartu 2000. 88 p.

61. **Dina Lepik.** Modulation of viral DNA replication by tumor suppressor protein p53. Tartu 2000. 106 p.
62. **Kai Vellak.** Influence of different factors on the diversity of the bryophyte vegetation in forest and wooded meadow communities. Tartu 2000. 122 p.
63. **Jonne Kotta.** Impact of eutrophication and biological invasionas on the structure and functions of benthic macrofauna. Tartu 2000. 160 p.
64. **Georg Martin.** Phytobenthic communities of the Gulf of Riga and the inner sea the West-Estonian archipelago. Tartu, 2000. 139 p.
65. **Silvia Sepp.** Morphological and genetical variation of *Alchemilla L.* in Estonia. Tartu, 2000. 124 p.
66. **Jaan Liira.** On the determinants of structure and diversity in herbaceous plant communities. Tartu, 2000. 96 p.
67. **Priit Zingel.** The role of planktonic ciliates in lake ecosystems. Tartu 2001. 111 p.
68. **Tiit Teder.** Direct and indirect effects in Host-parasitoid interactions: ecological and evolutionary consequences. Tartu 2001. 122 p.
69. **Hannes Kollist.** Leaf apoplastic ascorbate as ozone scavenger and its transport across the plasma membrane. Tartu 2001. 80 p.
70. **Reet Marits.** Role of two-component regulator system PehR-PehS and extracellular protease PrtW in virulence of *Erwinia Carotovora* subsp. *Carotovora*. Tartu 2001. 112 p.
71. **Vallo Tilgar.** Effect of calcium supplementation on reproductive performance of the pied flycatcher *Ficedula hypoleuca* and the great tit *Parus major,* breeding in Nothern temperate forests. Tartu, 2002. 126 p.
72. **Rita Hõrak.** Regulation of transposition of transposon Tn*4652* in *Pseudomonas putida*. Tartu, 2002. 108 p.
73. **Liina Eek-Piirsoo.** The effect of fertilization, mowing and additional illumination on the structure of a species-rich grassland community. Tartu, 2002. 74 p.
74. **Krõõt Aasamaa.** Shoot hydraulic conductance and stomatal conductance of six temperate deciduous tree species. Tartu, 2002. 110 p.
75. **Nele Ingerpuu.** Bryophyte diversity and vascular plants. Tartu, 2002. 112 p.
76. **Neeme Tõnisson.** Mutation detection by primer extension on oligonucleotide microarrays. Tartu, 2002. 124 p.
77. **Margus Pensa.** Variation in needle retention of Scots pine in relation to leaf morphology, nitrogen conservation and tree age. Tartu, 2003. 110 p.
78. **Asko Lõhmus.** Habitat preferences and quality for birds of prey: from principles to applications. Tartu, 2003. 168 p.
79. **Viljar Jaks.** p53 — a switch in cellular circuit. Tartu, 2003. 160 p.
80. **Jaana Männik.** Characterization and genetic studies of four ATP-binding cassette (ABC) transporters. Tartu, 2003. 140 p.
81. **Marek Sammul.** Competition and coexistence of clonal plants in relation to productivity. Tartu, 2003. 159 p

82. **Ivar Ilves.** Virus-cell interactions in the replication cycle of bovine papillomavirus type 1. Tartu, 2003. 89 p.
83. **Andres Männik.** Design and characterization of a novel vector system based on the stable replicator of bovine papillomavirus type 1. Tartu, 2003. 109 p.
84. **Ivika Ostonen.** Fine root structure, dynamics and proportion in net primary production of Norway spruce forest ecosystem in relation to site conditions. Tartu, 2003. 158 p.
85. **Gudrun Veldre.** Somatic status of 12–15-year-old Tartu schoolchildren. Tartu, 2003. 199 p.
86. **Ülo Väli.** The greater spotted eagle *Aquila clanga* and the lesser spotted eagle *A. pomarina*: taxonomy, phylogeography and ecology. Tartu, 2004. 159 p.
87. **Aare Abroi.** The determinants for the native activities of the bovine papillomavirus type 1 E2 protein are separable. Tartu, 2004. 135 p.
88. **Tiina Kahre.** Cystic fibrosis in Estonia. Tartu, 2004. 116 p.
89. **Helen Orav-Kotta.** Habitat choice and feeding activity of benthic suspension feeders and mesograzers in the northern Baltic Sea. Tartu, 2004. 117 p.
90. **Maarja Öpik.** Diversity of arbuscular mycorrhizal fungi in the roots of perennial plants and their effect on plant performance. Tartu, 2004. 175 p.
91. **Kadri Tali.** Species structure of *Neotinea ustulata*. Tartu, 2004. 109 p.
92. **Kristiina Tambets.** Towards the understanding of post-glacial spread of human mitochondrial DNA haplogroups in Europe and beyond: a phylogeographic approach. Tartu, 2004. 163 p.
93. **Arvi Jõers.** Regulation of p53-dependent transcription. Tartu, 2004. 103 p.
94. **Lilian Kadaja.** Studies on modulation of the activity of tumor suppressor protein p53. Tartu, 2004. 103 p.
95. **Jaak Truu.** Oil shale industry wastewater: impact on river microbial community and possibilities for bioremediation. Tartu, 2004. 128 p.
96. **Maire Peters.** Natural horizontal transfer of the *pheBA* operon. Tartu, 2004. 105 p.
97. **Ülo Maiväli.** Studies on the structure-function relationship of the bacterial ribosome. Tartu, 2004. 130 p.
98. **Merit Otsus.** Plant community regeneration and species diversity in dry calcareous grasslands. Tartu, 2004. 103 p.
99. **Mikk Heidemaa.** Systematic studies on sawflies of the genera *Dolerus, Empria,* and *Caliroa* (Hymenoptera: Tenthredinidae). Tartu, 2004. 167 p.
100. **Ilmar Tõnno.** The impact of nitrogen and phosphorus concentration and N/P ratio on cyanobacterial dominance and N_2 fixation in some Estonian lakes. Tartu, 2004. 111 p.
101. **Lauri Saks.** Immune function, parasites, and carotenoid-based ornaments in greenfinches. Tartu, 2004. 144 p.

102. **Siiri Rootsi.** Human Y-chromosomal variation in European populations. Tartu, 2004. 142 p.
103. **Eve Vedler.** Structure of the 2,4-dichloro-phenoxyacetic acid-degradative plasmid pEST4011. Tartu, 2005. 106 p.
104. **Andres Tover.** Regulation of transcription of the phenol degradation *pheBA* operon in *Pseudomonas putida*. Tartu, 2005. 126 p.
105. **Helen Udras.** Hexose kinases and glucose transport in the yeast *Hansenula polymorpha*. Tartu, 2005. 100 p.
106. **Ave Suija.** Lichens and lichenicolous fungi in Estonia: diversity, distribution patterns, taxonomy. Tartu, 2005. 162 p.
107. **Piret Lõhmus.** Forest lichens and their substrata in Estonia. Tartu, 2005. 162 p.
108. **Inga Lips.** Abiotic factors controlling the cyanobacterial bloom occurrence in the Gulf of Finland. Tartu, 2005. 156 p.
109. **Kaasik, Krista.** Circadian clock genes in mammalian clockwork, metabolism and behaviour. Tartu, 2005. 121 p.
110. **Juhan Javoiš.** The effects of experience on host acceptance in ovipositing moths. Tartu, 2005. 112 p.
111. **Tiina Sedman.** Characterization of the yeast *Saccharomyces cerevisiae* mitochondrial DNA helicase Hmi1. Tartu, 2005. 103 p.
112. **Ruth Aguraiuja.** Hawaiian endemic fern lineage *Diellia* (Aspleniaceae): distribution, population structure and ecology. Tartu, 2005. 112 p.
113. **Riho Teras.** Regulation of transcription from the fusion promoters generated by transposition of Tn*4652* into the upstream region of *pheBA* operon in *Pseudomonas putida*. Tartu, 2005. 106 p.
114. **Mait Metspalu.** Through the course of prehistory in india: tracing the mtDNA trail. Tartu, 2005. 138 p.
115. **Elin Lõhmussaar.** The comparative patterns of linkage disequilibrium in European populations and its implication for genetic association studies. Tartu, 2006. 124 p.
116. **Priit Kupper.** Hydraulic and environmental limitations to leaf water relations in trees with respect to canopy position. Tartu, 2006. 126 p.
117. **Heili Ilves.** Stress-induced transposition of Tn*4652* in *Pseudomonas Putida.* Tartu, 2006. 120 p.
118. **Silja Kuusk.** Biochemical properties of Hmi1p, a DNA helicase from *Saccharomyces cerevisiae* mitochondria. Tartu, 2006. 126 p.
119. **Kersti Püssa.** Forest edges on medium resolution landsat thematic mapper satellite images. Tartu, 2006. 90 p.
120. **Lea Tummeleht.** Physiological condition and immune function in great tits (*Parus major* l.): Sources of variation and trade-offs in relation to growth. Tartu, 2006. 94 p.
121. **Toomas Esperk.** Larval instar as a key element of insect growth schedules. Tartu, 2006. 186 p.

122. **Harri Valdmann.** Lynx (*Lynx lynx*) and wolf (*Canis lupus*) in the Baltic region: Diets, helminth parasites and genetic variation. Tartu, 2006. 102 p.
123. **Priit Jõers.** Studies of the mitochondrial helicase Hmi1p in *Candida albicans* and *Saccharomyces cerevisia*. Tartu, 2006. 113 p.
124. **Kersti Lilleväli.** Gata3 and Gata2 in inner ear development. Tartu, 2007. 123 p.
125. **Kai Rünk.** Comparative ecology of three fern species: *Dryopteris carthusiana* (Vill.) H.P. Fuchs, *D. expansa* (C. Presl) Fraser-Jenkins & Jermy and *D. dilatata* (Hoffm.) A. Gray (Dryopteridaceae). Tartu, 2007. 143 p.
126. **Aveliina Helm.** Formation and persistence of dry grassland diversity: role of human history and landscape structure. Tartu, 2007. 89 p.
127. **Leho Tedersoo.** Ectomycorrhizal fungi: diversity and community structure in Estonia, Seychelles and Australia. Tartu, 2007. 233 p.
128. **Marko Mägi.** The habitat-related variation of reproductive performance of great tits in a deciduous-coniferous forest mosaic: looking for causes and consequences. Tartu, 2007. 135 p.
129. **Valeria Lulla.** Replication strategies and applications of Semliki Forest virus. Tartu, 2007. 109 p.
130. **Ülle Reier**. Estonian threatened vascular plant species: causes of rarity and conservation. Tartu, 2007. 79 p.
131. **Inga Jüriado**. Diversity of lichen species in Estonia: influence of regional and local factors. Tartu, 2007. 171 p.
132. **Tatjana Krama.** Mobbing behaviour in birds: costs and reciprocity based cooperation. Tartu, 2007.
133. **Signe Saumaa.** The role of DNA mismatch repair and oxidative DNA damage defense systems in avoidance of stationary phase mutations in *Pseudomonas putida.* Tartu, 2007. 172 p.
134. **Reedik Mägi**. The linkage disequilibrium and the selection of genetic markers for association studies in european populations. Tartu, 2007. 96 p.
135. **Priit Kilgas.** Blood parameters as indicators of physiological condition and skeletal development in great tits (*Parus major*): natural variation and application in the reproductive ecology of birds. Tartu, 2007. 129 p.
136. **Anu Albert**. The role of water salinity in structuring eastern Baltic coastal fish communities. Tartu, 2007. 95 p.
137. **Kärt Padari.** Protein transduction mechanisms of transportans. Tartu, 2008. 128 p.
138. **Siiri-Lii Sandre.** Selective forces on larval colouration in a moth. Tartu, 2008. 125 p.
139. **Ülle Jõgar.** Conservation and restoration of semi-natural floodplain meadows and their rare plant species. Tartu, 2008. 99 p.
140. **Lauri Laanisto.** Macroecological approach in vegetation science: generality of ecological relationships at the global scale. Tartu, 2008. 133 p.
141. **Reidar Andreson**. Methods and software for predicting PCR failure rate in large genomes. Tartu, 2008. 105 p.

142. **Birgot Paavel.** Bio-optical properties of turbid lakes. Tartu, 2008. 175 p.
143. **Kaire Torn.** Distribution and ecology of charophytes in the Baltic Sea. Tartu, 2008, 98 p.
144. **Vladimir Vimberg.** Peptide mediated macrolide resistance. Tartu, 2008, 190 p.
145. **Daima Örd.** Studies on the stress-inducible pseudokinase TRB3, a novel inhibitor of transcription factor ATF4. Tartu, 2008, 108 p.
146. **Lauri Saag.** Taxonomic and ecologic problems in the genus *Lepraria* (*Stereocaulaceae*, lichenised *Ascomycota*). Tartu, 2008, 175 p.
147. **Ulvi Karu.** Antioxidant protection, carotenoids and coccidians in greenfinches – assessment of the costs of immune activation and mechanisms of parasite resistance in a passerine with carotenoid-based ornaments. Tartu, 2008, 124 p.
148. **Jaanus Remm.** Tree-cavities in forests: density, characteristics and occupancy by animals. Tartu, 2008, 128 p.
149. **Epp Moks.** Tapeworm parasites *Echinococcus multilocularis* and *E. granulosus* in Estonia: phylogenetic relationships and occurrence in wild carnivores and ungulates. Tartu, 2008, 82 p.
150. **Eve Eensalu.** Acclimation of stomatal structure and function in tree canopy: effect of light and CO_2 concentration. Tartu, 2008, 108 p.
151. **Janne Pullat**. Design, functionlization and application of an *in situ* synthesized oligonucleotide microarray. Tartu, 2008, 108 p.
152. **Marta Putrinš.** Responses of *Pseudomonas putida* to phenol-induced metabolic and stress signals. Tartu, 2008, 142 p.
153. **Marina Semtšenko.** Plant root behaviour: responses to neighbours and physical obstructions. Tartu, 2008, 106 p.
154. **Marge Starast.** Influence of cultivation techniques on productivity and fruit quality of some *Vaccinium* and *Rubus* taxa. Tartu, 2008, 154 p.
155. **Age Tats.** Sequence motifs influencing the efficiency of translation. Tartu, 2009, 104 p.
156. **Radi Tegova.** The role of specialized DNA polymerases in mutagenesis in *Pseudomonas putida.* Tartu, 2009, 124 p.
157. **Tsipe Aavik.** Plant species richness, composition and functional trait pattern in agricultural landscapes – the role of land use intensity and landscape structure. Tartu, 2008, 112 p.
158. **Kaja Kiiver.** Semliki forest virus based vectors and cell lines for studying the replication and interactions of alphaviruses and hepaciviruses. Tartu, 2009, 104 p.
159. **Meelis Kadaja.** Papillomavirus Replication Machinery Induces Genomic Instability in its Host Cell. Tartu, 2009, 126 p.
160. **Pille Hallast.** Human and chimpanzee Luteinizing hormone/Chorionic Gonadotropin beta (*LHB/CGB*) gene clusters: diversity and divergence of young duplicated genes. Tartu, 2009, 168 p.

161. **Ain Vellak.** Spatial and temporal aspects of plant species conservation. Tartu, 2009, 86 p.
162. **Triinu Remmel.** Body size evolution in insects with different colouration strategies: the role of predation risk. Tartu, 2009, 168 p.
163. **Jaana Salujõe.** Zooplankton as the indicator of ecological quality and fish predation in lake ecosystems. Tartu, 2009, 129 p.
164. **Ele Vahtmäe.** Mapping benthic habitat with remote sensing in optically complex coastal environments. Tartu, 2009, 109 p.
165. **Liisa Metsamaa.** Model-based assessment to improve the use of remote sensing in recognition and quantitative mapping of cyanobacteria. Tartu, 2009, 114 p.
166. **Pille Säälik.** The role of endocytosis in the protein transduction by cell-penetrating peptides. Tartu, 2009, 155 p.
167. **Lauri Peil.** Ribosome assembly factors in *Escherichia coli.* Tartu, 2009, 147 p.
168. **Lea Hallik.** Generality and specificity in light harvesting, carbon gain capacity and shade tolerance among plant functional groups. Tartu, 2009, 99 p.
169. **Mariliis Tark.** Mutagenic potential of DNA damage repair and tolerance mechanisms under starvation stress. Tartu, 2009, 191 p.
170. **Riinu Rannap.** Impacts of habitat loss and restoration on amphibian populations. Tartu, 2009, 117 p.
171. **Maarja Adojaan.** Molecular variation of HIV-1 and the use of this knowledge in vaccine development. Tartu, 2009, 95 p.
172. **Signe Altmäe.** Genomics and transcriptomics of human induced ovarian folliculogenesis. Tartu, 2010, 179 p.
173. **Triin Suvi.** Mycorrhizal fungi of native and introduced trees in the Seychelles Islands. Tartu, 2010, 107 p.
174. **Venda Lauringson.** Role of suspension feeding in a brackish-water coastal sea. Tartu, 2010, 123 p.